

© Copyright 2019

Julia Nguyen

Cross Coupling of Alkenyl Gold Complexes with Alkyl Electrophiles and Nickel
Catalyzed Hydroarylation of Alkenes

Julia Nguyen

A dissertation

submitted in partial fulfillment of the
requirements for the degree of

Doctor of Philosophy

University of Washington

2019

Reading Committee:

Gojko Lalic, Chair

Forrest Michael

Andrew J. Boydston

Program Authorized to Offer Degree:

Department of Chemistry

University of Washington

Abstract

Cross-Coupling of Alkenyl Gold Complexes with Alkyl Electrophiles and Nickel Catalyzed
Hydroarylation of Alkenes

Julia Nguyen

Chair of the Supervisory Committee:
Professor Gojko Lalic
Department of Chemistry

Transition metal catalysis is a powerful strategy for the construction of organic molecules. The development of novel methods in this field can help improve the speed and efficiency with which we synthesize complex organic molecules and broaden the scope of accessible products. Here we describe the development of two reactions involving transition metals. The first is a cross-coupling reaction between alkenyl gold and alkyl triflates, resulting in the formation of a new C-C bond. While several strategies are known that enable α -selective cross-coupling of alkenyl gold complexes, we are able to achieve β -selective cross-coupling by taking advantage of an alternative mode of reactivity. The second reaction described is a nickel catalyzed hydroarylation of alkenes. We are able to achieve good anti-Markovnikov selectivity with a wide range of alkenes, including styrenes, alkyl substituted alkenes, and enol ethers.

TABLE OF CONTENTS

List of Figures	iii
List of Schemes	iv
List of Tables	v
Chapter 1. Cross Coupling of Vinyl Gold(I) Complexes with Alkyl Triflates.....	1
1.1 Introduction.....	1
1.2 Results and Discussion	3
1.3 Conclusion	11
1.4 Experimental.....	12
1.4.1 General Information.....	12
1.4.2 Experimental Procedures	13
1.4.3 Synthesis and Characterization of Product Standards	14
1.4.4 Synthesis and Characterization of Organogold Complexes.....	24
1.4.5 Synthesis and Characterization of Alkyl Triflates	27
Chapter 2. Nickel Catalyzed Hydroarylation of Alkenes	28
2.1 Introduction.....	28
2.2 Reaction Optimization	30
2.3 Substrate Scope.....	34
2.4 Mechanistic Studies	38
2.5 Conclusion	43
2.6 Experimental.....	43

2.6.1	General Information.....	43
2.6.2	Reaction Development.....	44
2.6.3	General Procedure for the Hydroarylation of Alkenes	47
2.6.4	Characterization of Hydroarylation Products	47
2.6.5	Synthesis and Characterization of Alkene Starting Material.....	68
2.6.6	Mechanistic Experiments.....	76
	Bibliography	81

LIST OF FIGURES

Figure 1.1. Electrophilic interception of vinyl gold intermediate mediated by backbonding	3
Figure 1.2. Structure and yield of product B	8
Figure 1.3. Efforts to develop a gold catalyzed cross coupling reaction	10
Figure 2.1. Reductive cross-coupling of alkenes with aryl halides	29
Figure 2.2. A possible radical mechanism	38
Figure 2.3. Radical traps	38
Figure 2.4. A possible hydrometallation mechanism.....	39

LIST OF SCHEMES

Scheme 1.1. Reaction between 2-propenyl gold and alkyl triflate	4
Scheme 1.2. Formation and reactivity of alkenyl bis(gold) complex	5
Scheme 1.3. Reaction between ethenyl gold and alkyl triflate	6
Scheme 1.4. Reaction between (<i>E</i>)-alkenyl gold and alkyl triflate.....	7
Scheme 1.5. Reaction between more polar (<i>E</i>)-alkenyl gold and alkyl triflate and the subsequent deprotection of the products.....	7
Scheme 1.6. Reactivity of methyl and phenyl gold with alkyl triflate	9
Scheme 1.7. Possible mechanism for the formation of cyclopropane 18	9
Scheme 1.8. Reaction between α , β -disubstituted alkenyl gold and alkyl triflate	10
Scheme 1.9. Synthesis of (4 <i>E</i>)-[(4-hexenyl)oxy]triisopropylsilane 3	14
Scheme 1.10. Synthesis of (4 <i>Z</i>)-[(4-hexenyl)oxy]triisopropylsilane 31	15
Scheme 1.11. Synthesis of 1-(Trifluoromethyl)-4-[(4 <i>E</i>)-8-[(triisopropylsilyl)oxy]-4-octenyl]- benzene 14	17
Scheme 1.12. Synthesis of 1-(Trifluoromethyl)-4-[[trans-8-[(triisopropylsilyl)oxy]propyl]cyclopropylethyl]-benzene 18	20
Scheme 2.1. Proposed mechanism for hydroarylation of alkenes	30
Scheme 2.2. Stoichiometric nickel reactions	31
Scheme 2.3. Competition experiments	39
Scheme 2.4. Interception of alkyl nickel intermediate with EtOH.....	40
Scheme 2.5. Deuterium scrambling experiments	41
Scheme 2.6. Addition of mercury to reaction mixture.....	42

LIST OF TABLES

Table 2.1. Stoichiometric reactions between alkyl Ni 47 and electrophiles.....	32
Table 2.2. Nickel catalyzed hydroarylation reaction development ^a	33
Table 2.3. Alkene scope for nickel catalyzed hydroarylation ^a	36
Table 2.4. Aryl halide scope for nickel catalyzed hydroarylation ^a	37
Table 2.5. Ligand Screen	45
Table 2.6. Nickel Screen.....	45
Table 2.7. Solvent Screen	46
Table 2.8. Silane Screen.....	46
Table 2.9. TEMPO Experiments.....	80

ACKNOWLEDGEMENTS

First, I would like to thank my graduate advisor Gojko Lalic for all his support. I learned a lot during my time in graduate school and that would not have been possible without his mentorship. I would also like to thank all my lab mates past and present. Your camaraderie and friendship were essential in helping me get through the long hours in lab.

I would also like to thank all the friends I made during my time here. I feel very fortunate to have met a group of such generous and intelligent people and I look forward to seeing what the future has in store for all of you. I would especially like to thank Colin Liberty for frequently being a welcome distraction and for his unending support and encouragement.

Finally, I would like to thank my family for their love and support. This would not have been possible without them.

Chapter 1. CROSS COUPLING OF VINYL GOLD(I) COMPLEXES WITH ALKYL TRIFLATES

1.1 INTRODUCTION

Since the turn of the century, the development of homogeneous gold catalysis, particularly with Au(I) complexes, has been proceeding at a rapid rate.¹ Historically largely ignored, a seminal 1998 paper by Teles et al.² describing an Au(I) catalyzed hydration of alkynes demonstrated the potential of the field and marked the beginning of a 21st century “gold rush” as the advantages of gold over its metallic neighbors became apparent. Due to the high oxidation potential between Au(I) and Au(III), gold is resistant to, though capable of, the oxidative addition and reductive elimination processes that dominate transformations catalyzed by other late transition metals. As a result of this redox stability, gold complexes are often air and water stable, can tolerate a wide range of functional groups, and can access novel modes of reactivity orthogonal to that of other transition metal catalysts.³

The source of many of gold’s singular chemical properties are relativistic effects that, in short, result in the contraction of the 6s valence orbital. The contraction of the s orbital results in a relatively low energy lowest unoccupied molecular orbital (LUMO) and makes gold a particularly good Lewis acid.⁴ Due to this superior Lewis acidity, an often invoked mode of reactivity for Au(I) catalysis is activation of a carbon-carbon π -system, such as alkyne, allenes, and alkenes, towards nucleophilic addition.⁵ Belying the wide variety of products accessible through this reactivity is the fact that many of these reactions proceed through an alkenyl gold intermediate.⁶ In a vast majority of reactions, the alkenyl gold complex either undergoes protodeauration or is intercepted by an electrophile in an intramolecular reaction.⁷ More recently,

several examples of intermolecular interception of alkenyl gold intermediates have been reported, further expanding the scope and utility of gold catalysis. These methods enable direct cross-coupling of alkenyl gold intermediates and lead to the formation of a new carbon-carbon bond.

So far, three strategies have been developed to achieve cross-coupling reactions of alkenyl gold complexes. One approach is to use a second metal, such as palladium or nickel, to catalyze cross-coupling between alkenyl gold complexes and an organohalide, such as aryl iodide, acyl chloride, and methyl iodide.⁸ Another method is to access Au(I)/Au(III) redox cycles using a strong oxidant, such as Selectfluor. This strategy has been successfully applied to homocoupling⁹ and to cross-coupling with aryl boronic acids.¹⁰ The third approach also involves Au(I)/Au(III) redox cycles, but instead of a stoichiometric oxidant, a ruthenium photoredox catalyst is used to generate a Au(III) species. This dual gold-ruthenium catalytic system has been used to accomplish coupling of alkenyl gold intermediates with aryl diazonium salts.¹¹

All three strategies for cross-coupling of alkenyl gold complexes have been mostly focused on aryl and acyl coupling partners, generating C(sp²)-C(sp²) bonds. Exceptions are methyl and allyl electrophiles, which have been used palladium-catalyzed cross-coupling of alkenyl gold complexes.²⁷ Another common feature of these three strategies is that the new C-C bond is formed at the α carbon of the alkenyl gold complex.

The unique relativistic effects in play with gold suggest another possible mode of reactivity and an opportunity to change the regioselectivity and expand the scope of cross-coupling reactions with alkenyl gold complexes. Besides increasing gold's Lewis acidity, the contracted s orbitals better shield the d orbitals from the nucleus, and as a result, these d orbitals are expanded.⁴ In alkenyl gold species, the relativistically expanded 6d orbitals can facilitate trapping of an electrophile at the β carbon of alkenyl gold complexes through backbonding (Fig 1.1). After a

hydride shift, the resulting gold carbenoid provides the desired alkene product. This mode of reactivity has been postulated in several examples of intramolecular reactions of alkenyl gold complexes with electrophiles.³⁰⁻³² Inspired by these examples, we hypothesized that the same reactivity could be achieved intermolecularly using a particularly good electrophile. Here, we describe a method for the β -selective cross-coupling of alkenyl gold complexes with simple alkyl triflates. We also show that the mode of reactivity of alkenyl gold complexes with alkyl triflates varies dramatically as we change electronic and steric properties of the gold complexes.¹³

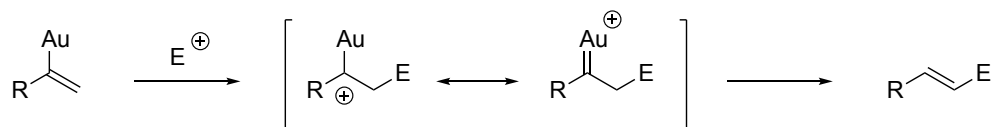
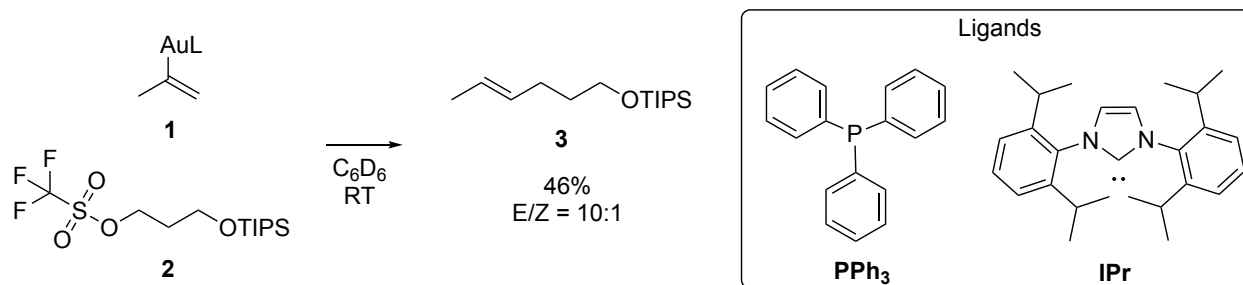


Figure 1.1. Electrophilic interception of vinyl gold intermediate mediated by backbonding

1.2 RESULTS AND DISCUSSION

For our initial reactions, we combined a vinyl gold complex and a triflate in a sealed NMR tube and observed the solution by NMR over time to determine if the desired reaction occurred at all. Using dioctyl ether as a standard and alkyl triflate **2**, we first attempted the reaction with vinyl gold complexes of type **1** where triphenylphosphine was the ligand (Scheme 1.1). Despite trying a variety of solvents, (benzene, dichloromethane, chloroform, and dimethylsulfoxide) at a variety of temperatures, from 20 °C to 100 °C, expected product **3** was not detected by NMR or GC-MS. Rather, the protodeauration product ethylene and the triflate elimination product were detected by NMR.



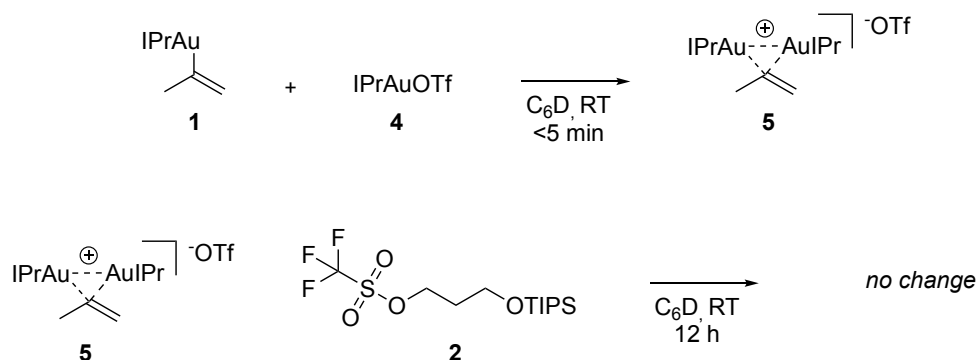
Scheme 1.1. Reaction between 2-propenyl gold and alkyl triflate

Hypothesizing that a better σ donor ligand was needed to increase the electron density on the gold center, we switched to *N,N'*-bis(2,6-diisopropylphenyl)-imidazol-2-ylidene (IPr) supported complexes.¹⁴ This change proved to be constructive, and treatment of alkenyl gold complex **1** with alkyl triflate **2** in C_6D_6 at room temperature generated the expected alkene product **3**, with the *E* isomer being the major product (Scheme 1.1). Though initially product formation occurs relatively rapidly, upon approaching 50% yield, the rate of product formation dramatically decreases and the final yield generally does not rise above 50%. Curiously, 1H NMR showed complete consumption of the alkenyl gold **1** after approximately 25 hours and there was no evidence of the protodeauration product, propylene. We made several efforts to increase the yield, including a solvent screen, increasing the temperature, increasing the equivalents of alkyl triflate, and addition 2,6-lutidine as a proton scavenger. None of these changes significantly increased yield of the desired product.

While monitoring the reaction by 1H NMR, we had observed the appearance of two doublets between 4.3 to 4.6 ppm, which grew during the start of the reaction and disappeared towards the end. This development was accompanied by the formation of a white solid in the NMR tube. We suspected that those peaks corresponded to alkenyl bis(gold) complex **5** and disappeared as **5** crystallized out of solution to form the white solid. Alkenyl bis(gold) complex **5** could be generated by a reaction between IPrAuOTf **4**, a presumed product of the reaction between

alkenyl gold and alkyl triflate, and alkenyl gold **1**. To test this hypothesis, alkenyl gold **1** and excess **4** were combined in C_6D_6 , and based on 1H NMR, **1** was completely consumed within 5 minutes (Scheme 1.2). 1H NMR spectrum of the newly formed complex featured the characteristic doublets we had previously observed in a reaction shown in Scheme 1.1. X-ray crystallography confirmed the structure of complex **5**.

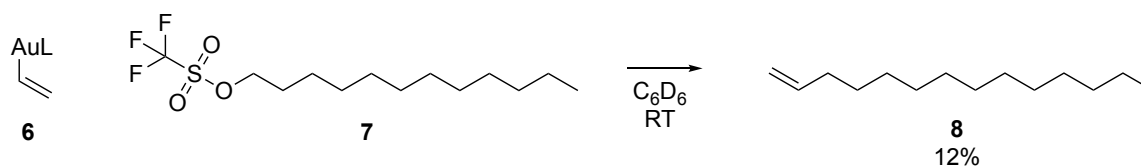
Hypothesizing that the low yield of the cross-coupling product in the reaction shown in Scheme 1.2 is due to the lower nucleophilicity of the alkenyl (bis)gold species **5**, we treated **5** with alkyl triflate **2** and did not observe significant product formation after 4 days. These results suggest that $IPrAuOTf$ **4**, which is formed as a side product of the alkenyl gold and alkyl triflate reaction, can sequester any remaining alkenyl gold species **1** through the generation of (bis)gold species **5**, thus limiting yields of the final alkene product to around 50%.



Scheme 1.2. Formation and reactivity of alkenyl bis(gold) complex

Formation of unreactive alkenyl (bis)metal species have several precedents in the literature. Previous work in our lab had found that in stoichiometric reactions between alkenyl Cu complex and alkyl triflate, formation of a dinuclear alkenyl copper complex also limited the yield of the desired product to approximately 50%.¹⁵ Additionally, Widenhoefer et al. found an alkenyl bis(gold) species to be an off cycle catalyst reservoir in their gold catalyzed allene

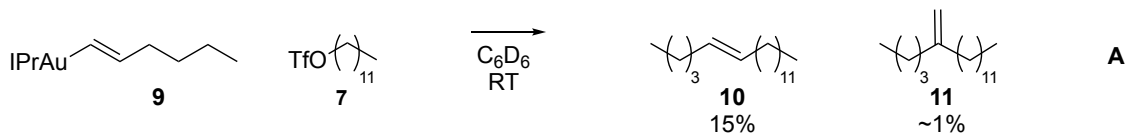
hydroalkoxylation reaction.¹⁶ Notably, in these examples, formation of an alkenyl bis(metal) species was not found to significantly detract from the yield in catalytic reactions. Thus, the reactivity revealed in this stoichiometric study of alkenyl gold and alkyl triflate offers insight for the development of a catalytic reaction that does not need to be limited by the formation of bis(gold) complexes.



Scheme 1.3. Reaction between ethenyl gold and alkyl triflate

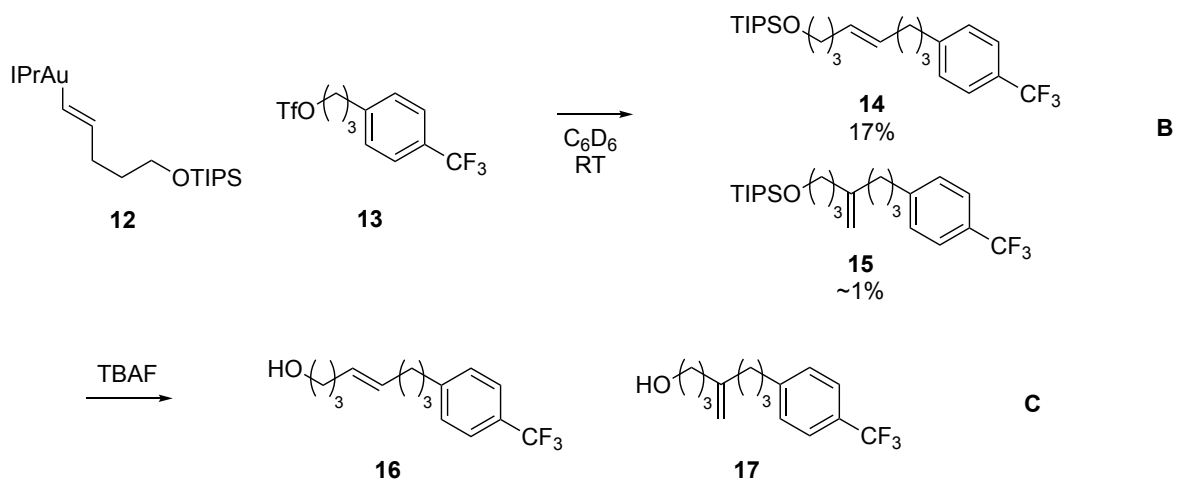
Having confirmed that alkyl triflate can intercept 2-propenyl gold, we next explored the scope of alkenyl gold species that can undergo this electrophilic interception. Treatment of ethenyl gold **6** with dodecyl triflate **7** afforded expected alkene product **8** (Scheme 1.3). Interestingly, both the yield and rate of the reaction were significantly reduced as compared to those of the 2-propenyl gold complex reaction (Scheme 1.1). It seems that the additional methyl on the 2-propenyl gold complex plays an important role in facilitating electrophilic interception, possibly by stabilizing the cationic intermediate generated upon trapping of the alkenyl gold species (Fig. 1.1).

Both the 2-propenyl gold **1** and ethenyl gold **6** contain a terminal alkene, and we know for complex **1**, and it is possible for complex **6**, that the new C-C bond is formed on the less hindered β carbon. We were curious as to whether adding steric hindrances to that β carbon would effect the product distribution of the cross coupling reaction. Based on product **3** from the 2-propenyl gold reaction and the mechanism detailed in Fig. 1, we would expect the generation of a 1,1-disubstituted alkene in a reaction between a linear alkenyl gold species and an alkyl triflate.



Scheme 1.4. Reaction between (*E*)-alkenyl gold and alkyl triflate

We synthesized alkenyl gold complex **9** and combined it with dodecyl triflate **7** (Fig 1.4). Based on GC/MS, three products were formed and all had the same molar mass. Surprisingly, the expected 1,1 disubstituted alkene product was a very minor product, with around a 1% yield. The other two products were both formed in significantly higher yields. We confirmed that one of the products was (*E*)-alkene **10** by synthesizing an authentic sample of that alkene and comparing it with the reaction mixture. The identity of the third product, **A**, whose yield based on GC was similar to that of the (*E*)-alkene, eluded us. Comparison of the reaction mixture and an authentic sample of the *Z* isomer of **10** eliminated such an isomer as a possibility. A lower than expected integration of the vinylic region of the ^1H NMR suggested that perhaps **A** was a reduced version of **13**, but GC comparison of an authentic sample of reduced product suggests that this was not the case.



Scheme 1.5. Reaction between more polar (*E*)-alkenyl gold and alkyl triflate and the subsequent deprotection of the products

We attempted to purify the products of our reaction mixture, but given greasy nature of both our starting materials and all the products, we had a hard time getting any separation at all by column chromatography. Everything seemed to move with the solvent front even though our solvent was simply hexanes. Hoping to get better separation, a few polar triflates and alkenyl gold compounds were screened before alkenyl gold complex **12** and alkyl triflate **13** were chosen (Scheme 1.5). After coupling **12** and **13**, the products were deprotected with tetra-*n*-butylammonium fluoride (TBAF) to give alcohols **16**, **17** and **C**. Unfortunately, separation of these products defied column chromatography and preparatory liquid chromatography efforts. However, we were able to obtain a relatively clean ^1H NMR and COSY NMR of the mixture of **16**, **17** and **C**, and the spectra suggested that unknown product **C** contained a cyclopropyl group. We synthesized compound **18** (Fig. 1.2) and its cis isomer and compared them to the reaction mixture of **14**, **15** and **B**. The ^1H NMR shifts and GC retention times of **B** are consistent with compound **18** and interestingly, there does not seem to be evidence of significant formation of its cis isomer.

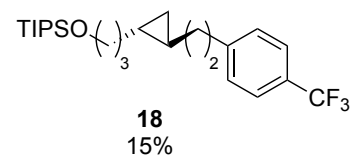
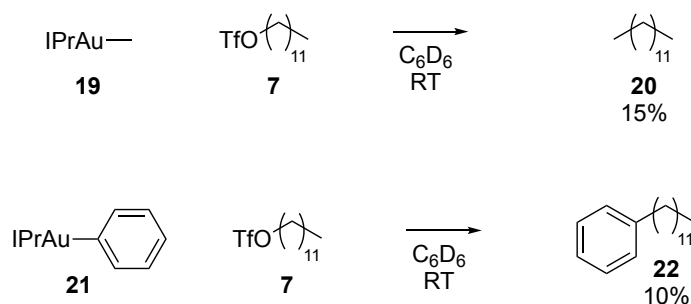


Figure 1.2. Structure and yield of product **B**

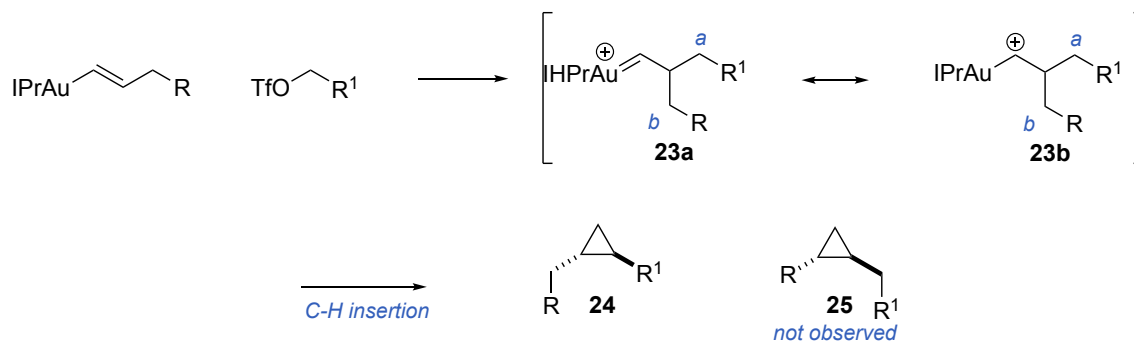
Both of the major products for the reaction between (*E*)-alkenyl gold and alkyl triflate are unlikely to be formed by the mechanism outlined in Fig. 1.1. We hypothesize that steric hinderance on the β carbon of alkenyl gold may making other mechanisms more favorable. A plausible mechanism for the formation of alkene **10** is an oxidative addition/reductive elimination sequence. In a classic paper by Kochi et al., methyl Au(I) was found to cross-couple with MeI in a sequence that involves oxidative addition and reductive elimination.¹⁷ Formation of compound

10 through an oxidative addition/reductive elimination mechanism is consistent with the generation of a C-C bond at the α -carbon and the conservation of the double bond geometry seen in product **10**. In addition, we were able to achieve cross coupling of methyl gold and phenyl gold with alkyl triflate, both of which could be formed through an oxidative addition/reductive elimination mechanism (Scheme 1.6)



Scheme 1.6. Reactivity of methyl and phenyl gold with alkyl triflate

A plausible mechanism for the formation of cyclopropane **18** is shown in Scheme 1.7, and involves the formation of a gold carbenoid intermediate, followed by a C-H insertion reaction. While the insertion is possible at both positions *a* and *b* (products **24** and **25**, respectively), only the product from the insertion at position *a* has been observed in reaction shown in Scheme 1.5. This selectivity of the proposed C-H insertion step is difficult to explain.



Scheme 1.7. Possible mechanism for the formation of cyclopropane **18**

1.3A). We replace the alcohol with an aryl nucleophile in the hopes that it would not be nucleophilic enough to react with the triflate. However, gold is known to be able to cross coupling with terminal alkynes¹⁸ and we obtained the disubstituted alkyne product instead (Fig. 1.3B). Switching out the alkyne for an allene allowed us to avoid that cross coupling reaction. However, by ¹H NMR, no reaction occurred with 2,6-lutidine as a base. Concerned that 2,6-lutidine was coordinating with the IPrAuTf catalyst and deactivating it, we tried a variety of other bases, including triethyl amine, sodium bicarbonate, a proton sponge, N,N-diisopropylamine, and N,N-dicyclohexylamine, but these bases would either react with the triflate or no reaction would occur (Fig. 1.3C). To avoid the issue of having a base entirely, we envisioned using a silyl ketene acetal as the nucleophile such that no proton would be produced in the course of the reaction. Unfortunately, we found that the alkyl triflate reacts unproductively with the silylketene acetal and we had difficulties installing an allene onto such a substrate (Fig. 1.3D)

1.3 CONCLUSION

In summary, we describe the reactions of various alkenyl gold complexes with alkyl triflates. We demonstrated that the efficiency and product distribution of the reaction strongly depends on the structure of gold complexes. With α -substituted alkenyl gold complexes, an efficient and highly β -selective cross-coupling is observed, together with the formation of the dinuclear alkenyl gold complex. The substitution at the α position facilitates the cross-coupling reaction, presumably by stabilizing the cationic intermediate. Substitution at the β position, on the other hand, hinders the β -selective cross-coupling, presumably through steric hindrance. Overall, reactions with alkyl triflates broaden the synthetic potential of alkenyl gold intermediates, which

are ubiquitous in the field of homogeneous gold catalysis, and provide an opportunity for the development of new catalytic processes.

1.4 EXPERIMENTAL

1.4.1 *General Information*

All reactions were performed under a nitrogen atmosphere with flame-dried glassware, using standard Schlenk technique, or in a glove box (Nexus II from Vacuum Atmospheres). Column chromatography was performed using a Biotage Iso-1SV flash purification system with silica gel from Agela Technologies Inc. (60Å, 40-60 µm, 230-400 mesh). Infrared (IR) spectra were recorded on a Perkin Elmer Spectrum RX I spectrometer. IR peak absorbencies are represented as follows: s = strong, m = medium, w = weak, br = broad. ¹H- and ¹³C-NMR spectra were recorded on a Bruker AV-300 or AV-500 spectrometer. ¹H NMR chemical shifts (δ) are reported in parts per million (ppm) downfield of TMS and are referenced relative to residual protiated solvent peak (CDCl₃ (7.26 ppm) or C₆D₆ (7.16 ppm)). ¹³C chemical shifts are reported in parts per million downfield of TMS and are referenced to the carbon resonance of the solvent (CDCl₃ (77.2 ppm) or C₆D₆ (128.1 ppm)). Data are represented as follows: chemical shift, multiplicity (s = singlet, d = doublet, t = triplet, q = quartet, quin = quintet, sept = septet, m = multiplet), integration, and coupling constants in Hertz (Hz). Mass spectra were collected on a JEOL HX-110 mass spectrometer. GC analysis was performed on a Shimadzu GC-2010 instrument with a flame ionization detector and a SHRXI-5MS column (15 m, 0.25 mm inner diameter, 0.25 µm film thickness). The following temperature program was used: 2 min @ 60 °C, 13 °C/min to 160 °C, 30 °C/min to 250 °C, 5.5 min @ 250 °C.

Materials: Toluene, benzene, ether, DCM, and THF were degassed and dried by passing through columns of neutral alumina. 1,4-Dioxane was distilled from purple Na/benzophenone ketyl and stored over 4Å molecular sieves. All other solvents were used as received. Deuterated solvents were purchased from Cambridge Isotope Laboratories, Inc. Deuterated solvents were degassed and dried over 4Å molecular sieves before use. Commercial reagents were purchased from Sigma-Aldrich Co., VWR International, LLC., TCI Chemicals USA, or STREM Chemicals, Inc., and were used as received. IPrAuCl was prepared from commercially available Me₂SAuCl (Sigma Aldrich) according to a reported procedure. IPrAuOTf was prepared from IPrAuCl according to a reported procedure.

1.4.2 *Experimental Procedures*

General Procedure for the Electrophilic Interception of Organogold by Alkyl Triflate

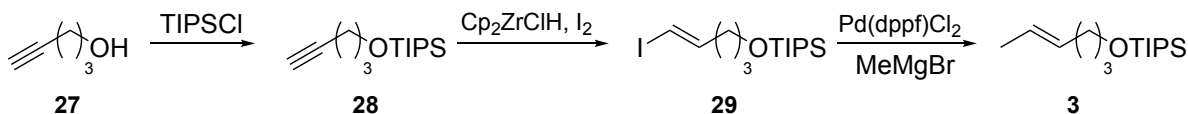
In a N₂ filled glovebox, organogold complex (1 equiv) was weighed into a dram vial. Alkyl triflate (2 equiv), methyl 4-methoxybenzoate standard (0.50 equiv) and 0.6 mL of C₆D₆ were added to the dram vial. The contents of the dram vial were then transferred to a J. Young tube with a Teflon plug valve. The reaction mixture was left to sit in the dark until ¹H-NMR showed complete consumption of the vinyl gold complex.

Formation of Alkenyl Bis(gold)complex

In a scintillation vial, IPr(propenyl)Au (32.4 mg, 1.0 equiv, 0.045 mmol), IPrAuOTf (31.3 mg, 1.1 equiv, 0.050 mmol) and benzene (0.45 mL, 0.10 M) were added. The solution was left to sit in the dark overnight, after which alkenyl bis(gold)complex was found at the bottom of the scintillation vial as clear, colorless crystals.

1.4.3 Synthesis and Characterization of Product Standards

To identify the products of the alkenyl gold and alkyl triflate reaction, we synthesized the expected products independently and compared these compounds with those produced in the reaction through ^1H NMR and GC/MS.



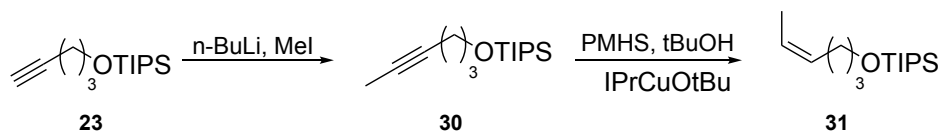
Scheme 1.9. Synthesis of (4E)-[(4-hexenyl)oxy]triisopropylsilane **3**

[(4-Pentynyl)oxy]triisopropylsilane (28). Sodium hydride (960 mg, 1.2 equiv, 24 mmol) was suspended in THF (40 mL, 0.5 M) after being washed with hexane. 4-Pentyn-1-ol (2.2 mL, 1 equiv, 20 mmol) was added to this mixture at room temperature and stirred for 45 min at which time a large amount of an opaque white precipitate had formed. Triisopropylsilyl chloride (3.2 mL, 1.2 equiv, 24 mmol) was then added, and vigorous stirring was continued for 45 min. The mixture was poured into ether, washed with 10% aqueous K_2CO_3 and brine, dried with MgSO_4 , and concentrated in vacuo. The crude product was purified by flash chromatography (SiO_2 : hexanes) to obtain 3.6 g (14 mmol, 71%) of [(4-pentynyl)oxy]triisopropylsilane as a clear colorless oil. ^1H NMR (300 MHz, CDCl_3) δ 3.77 (t, $J = 6.0$ Hz, 2H), 2.31 (td, $J = 7.1, 2.6$ Hz, 2H), 1.93 (t, $J = 2.7$ Hz, 1H), 1.86 – 1.63 (m, 2H), 1.18 – 0.95 (m, 21H).

(4E)-[(5-iodo-4-pentenyl)oxy]triisopropylsilane (29). To a solution of [(4-pentynyl)oxy]triisopropylsilane (480 mg, 1 equiv, 2 mmol) and Cp_2ZrCl_2 (640 mg, 1.1 equiv, 2.2 mmol) in THF (4 mL, 0.5 M) at rt was rapidly added a 1 M THF solution of $\text{LiAlH}(\text{O}t\text{-Bu})_3$ (2.2 mL, 1.4 equiv, 2.8 mmol, 1.0 M). The resulting mixture was stirred at rt for 15 min. Then, a solution of iodine (1.4 equiv) in THF was added. After additional stirring at rt for 15 min, the reaction mixture was

quenched with a solution of 1 N HCl and extracted with diethyl ether. The combined organic extract was washed successively with saturated Na₂SO₃, dried with MgSO₄ and concentrated under vacuum. The residue was subjected to flash chromatography (SiO₂: hexanes) to yield 310 mg (0.8 mmol, 42%) of (4*E*)-[(5-iodo-4-pentenyl)oxy]triisopropylsilane. ¹H NMR (300 MHz, CDCl₃) δ 6.52 (dt, *J* = 14.3, 7.1 Hz, 1H), 5.98 (dt, *J* = 14.3, 1.4 Hz, 1H), 3.67 (t, *J* = 6.1 Hz, 2H), 2.08 (td, *J* = 7.1, 5.9 Hz, 2H), 1.64 – 1.37 (m, 6H), 1.19 – 0.96 (m, 26H).

(4*E*)-[(4-hexenyl)oxy]triisopropylsilane (3). To a flame dried flask under nitrogen was added (4*E*)-[(5-iodo-4-pentenyl)oxy]triisopropylsilane (310 mg, 1 equiv, 0.8 mmol), [1,1'-Bis(diphenylphosphino)ferrocene]dichloropalladium(II) (13 mg, 0.02 equiv, 0.016 mmol), methylmagnesium bromide (0.4 mL, 1.5 equiv, 1.2 mmol, 3 M) and THF (1.6 mL, 0.5 M). After additional stirring at rt overnight, the reaction mixture was quenched with a solution of 1 N HCl and extracted with DCM. The organic extract was dried with MgSO₄ and concentrated under vacuum. The residue was subjected to flash chromatography (SiO₂: hexanes) to yield 97 mg (0.36 mmol, 45%) of (4*E*)-[(4-hexenyl)oxy]triisopropylsilane. ¹H NMR (500 MHz, CDCl₃) δ 5.52 – 5.35 (m, 2H), 3.67 (t, *J* = 6.5 Hz, 2H), 2.09 – 1.99 (m, 2H), 1.68 – 1.48 (m, 5H), 1.14 – 0.96 (m, 21H). ¹³C NMR (75 MHz, CDCl₃) δ 131.3, 125.1, 77.6, 77.2, 76.8, 63.0, 33.1, 29.1, 18.2, 18.10, 12.2. GC/MS calculated for [M]⁺ 255.5, found 255.3. FTIR (neat, cm⁻¹): 3021 (m), 2940 (s), 2867 (s), 1642 (w), 1465 (s), 1104 (s), 964 (s), 882 (s).

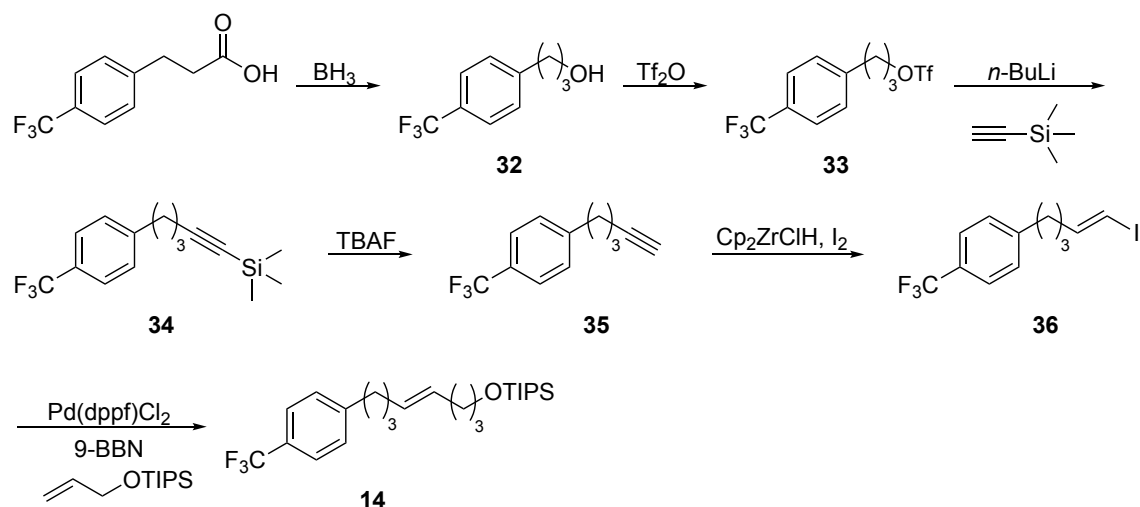


Scheme 1.10. Synthesis of (4*Z*)-[(4-hexenyl)oxy]triisopropylsilane **31**

[(4-Hexynyl)oxy]triisopropylsilane (30). To a solution of [(4-pentynyl)oxy]triisopropylsilane (480 mg, 1 equiv, 2 mmol) and dry THF (4 mL, 0.5 M) under N₂ was added dropwise *n*-BuLi in hexanes (2.5 M, 1.6 mL, 2 equiv, 4 mmol) at 0 °C. After the solution was stirred for 1.5 h, MeI (0.25 mL, 2 equiv, 4 mmol) and dimethyl-*N,N'*-trimethyleneurea were added. The reaction mixture was warmed to rt and left to stir overnight. The reaction was then quenched with water and extracted with DCM. The organic extract was dried with MgSO₄ and concentrated under vacuum. The crude product was purified by flash chromatography (SiO₂: hexanes) to obtain 260 mg (1.0 mmol, 51%) of [(4-hexynyl)oxy]triisopropylsilane as a clear colorless oil. ¹H NMR (300 MHz, CDCl₃) δ 3.75 (t, *J* = 6.1 Hz, 2H), 2.30 – 2.15 (m, 2H), 1.84 – 1.61 (m, 5H), 1.18 – 0.94 (m, 21H).

(4Z)-[(4-hexenyl)oxy]triisopropylsilane (31). In a glove box, a dram vial equipped with a stir bar was charged with [(4-hexynyl)oxy]triisopropylsilane (260 mg, 1.00 equiv, 1.0 mmol), polymethylhydrosiloxane (66 μL, 1.2 equiv, 1.2 mmol), toluene (1 mL, 0.5 M), and tert-butanol (0.11 mL, 1.2 equiv, 1.2 mmol). IPrCuOt-Bu (21 mg, 0.04 equiv, 0.04 mmol) was added and the reaction mixture was stirred for 8 h at 40 °C in a capped vial. The crude product was purified by flash chromatography (SiO₂: hexanes) to obtain 76 mg (0.29 mmol, 30%) of (4Z)-[(4-hexenyl)oxy]triisopropylsilane as a clear colorless oil. ¹H NMR (300 MHz, CDCl₃) δ 5.74 – 5.49 (m, 2H), 3.89 (t, *J* = 6.5 Hz, 2H), 2.41 – 2.23 (m, 2H), 1.91 – 1.71 (m, 5H), 1.35 – 1.20 (m, 21H). ¹³C NMR (75 MHz, C₆D₆) δ 130.5, 124.3, 77.6, 77.2, 76.8, 63.1, 33.1, 23.4, 18.2, 12.9, 12.3. GC/MS calculated for [M]⁺ 255.5, found 255.1. FTIR (neat, cm⁻¹): 3014 (m), 2944 (s), 2866 (s), 1656 (w), 1465 (m) 1110 (s), 882 (s).

1-Tetradecene (8) was purchased from Sigma-Aldrich and used as received.



Scheme 1.11. Synthesis of 1-(Trifluoromethyl)-4-[(4E)-8-[(triisopropylsilyl)oxy]-4-octenyl]-benzene **14**

3-(4-Trifluoromethylphenyl)-1-propanol (28). 4-(Trifluoromethyl)hydrocinnamic acid (2.0 g, 1.0 equiv, 9.2 mmol) was dissolved in tetrahydrofuran (23 mL, 0.4 M) and cooled to 0 °C. A borane tetrahydrofuran complex solution (1 M, 14 mL, 1.5 equiv, 14 mmol) was then added dropwise and the reaction mixture was stirred at rt for 16 h. The reaction was quenched with water and extracted with DCM. The organic extract was dried with MgSO₄ and concentrated under vacuum to give 1.9 g (9.2 mmol, 100%) of 3-(4-trifluoromethylphenyl)-1-propanol as a clear colorless oil. ¹H NMR (500 MHz, CDCl₃) δ 7.54 (d, *J* = 8.0 Hz, 2H), 7.31 (d, *J* = 7.9 Hz, 2H), 3.68 (t, *J* = 6.3 Hz, 2H), 2.78 (t, *J* = 7.7 Hz, 2H), 1.96 – 1.85 (m, 2H), 1.42 (s, 1H).

3-(4-Trifluoromethylphenyl)-1-propyl trifluoromethanesulfonate (29). To a flame-dried reaction flask under N₂ was added (4-trifluoromethylphenyl)-1-propanol (610 mg, 1.0 equiv, 3.0 mmol), DCM (6.0 mL, 0.5 M), and 2,4-lutidine (0.55 mL, 1.6 equiv, 4.8 mmol). The reaction mixture was cooled to -78 °C and triflic anhydride (0.55 mL, 1.1 equiv, 3.3 mmol) was added dropwise. The mixture was left to stir at -78 °C for 30 min. Then, 20 mL of hexanes was added

to the reaction flask and the mixture was poured onto a silica gel plug and the plug was washed with a 20:80 mixture of ethyl acetate:hexane. The filtrate was concentrated under vacuum to give 960 mg (2.9 mmol, 95%) of 3-(4-trifluoromethylphenyl)-1-propyl trifluoromethanesulfonate as a clear colorless oil. ^1H NMR (300 MHz, CDCl_3) δ 7.58 (d, $J = 8.1$ Hz, 2H), 7.31 (d, $J = 8.0$ Hz, 2H), 4.54 (t, $J = 6.1$ Hz, 2H), 2.85 (t, $J = 7.6$ Hz, 2H), 2.28 – 2.09 (m, 2H).

1-[(5-Triethylsilyl)pentyn-4-yl]-4-trifluoromethylbenzene (30). A solution of ethynyl trimethylsilane (0.28 mL, 1.2 equiv, 2.0 mmol) in THF (4.0 mL, 0.5 M) was cooled to -78 °C. *n*-BuLi (2.5 M, 0.67 mL, 1 equiv, 1.7 mmol) was added dropwise. The mixture was warmed to 0 °C and left to stir for 30 min. The reaction mixture was then cooled to -78 °C and 3-(4-trifluoromethylphenyl)-1-propyl trifluoromethanesulfonate (560 mg, 1 equiv, 1.7 mmol) was added. The reaction was warmed to 0 °C and left to stir for 1 h. Then, water was added to quench the reaction and the product was extracted with DCM. The organic extract was dried with MgSO_4 and concentrated under vacuum. The crude product was purified by flash chromatography (SiO_2 : hexanes) to obtain 300 mg (1.1 mmol, 63%) of 1-[(5-triethylsilyl)pentyn-4-yl]-4-trifluoromethylbenzene. ^1H NMR (300 MHz, CDCl_3) δ 7.54 (d, $J = 8.0$ Hz, 2H), 7.30 (d, $J = 8.0$ Hz, 2H), 2.78 (t, $J = 7.5$ Hz, 2H), 2.24 (t, $J = 7.0$ Hz, 2H), 1.94 – 1.72 (m, 2H), 0.17 (s, 9H).

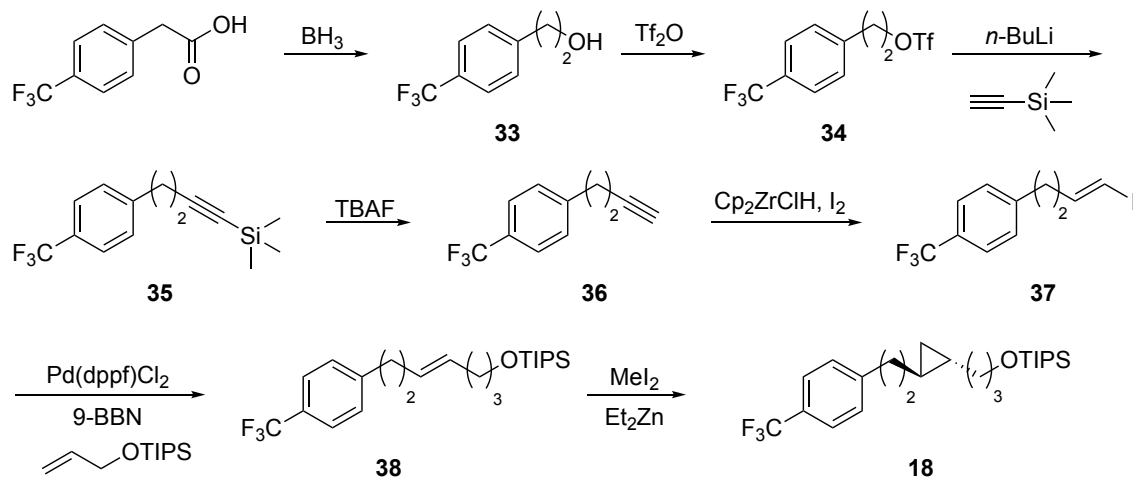
[1-(4-Pentynyl)-4-trifluoromethyl] benzene (31). In a round bottom flask, 1-[(5-triethylsilyl)pentyn-4-yl]4-trifluoromethylbenzene (280 mg, 1 equiv, 1 mmol) and tetra-*n*-butylammonium fluoride (1.0 M, 2.0 mL, 2 equiv, 2.0 mmol) were added. The mixture was stirred for 1 hour before water was added. The aqueous mixture was extracted with DCM. The organic extract was dried with MgSO_4 and concentrated under vacuum. The crude product was purified by flash chromatography (SiO_2 : hexanes) to obtain 200 mg (0.77 mmol, 77%) of [1-(4-pentynyl)-4-

trifluoromethyl] benzene. ^1H NMR (300 MHz, CDCl_3) δ 7.54 (d, $J = 8.0$ Hz, 2H), 7.31 (d, $J = 8.0$ Hz, 2H), 2.80 (t, $J = 7.6$ Hz, 2H), 2.21 (td, $J = 6.9, 2.5$ Hz, 2H), 2.01 (t, $J = 2.6$ Hz, 1H), 1.94 – 1.72 (m, 2H).

(4E)-1-(5-Iodo-4-pentenyl)-4-trifluoromethylbenzene (32). To a solution of 1-(4-pentynyl)-4-trifluoromethylbenzene (170 mg, 1 equiv, 0.82 mmol) and Cp_2ZrCl_2 (260 mg, 1.1 equiv, 0.90 mmol) in THF (1.6 mL, 0.5 M) at rt was rapidly added a solution of $\text{LiAlH}(\text{Ot-Bu})_3$ in THF (1 M, 0.90 mL, 1.1 equiv, 0.90 mmol). The resulting mixture was stirred at rt for 15 min. Then, a solution of I_2 (230 mg, 1.1 equiv, 0.90 mmol) in THF was added. After additional stirring at rt for 15 min, the reaction mixture was quenched with a solution of 1 N HCl and extracted with diethyl ether. The combined organic extract was washed successively with saturated Na_2SO_3 , dried with MgSO_4 and concentrated under vacuum. The residue was subjected to flash chromatography (SiO_2 : hexanes) to yield 150 mg (0.43 mmol, 52%) of (4E)-1-(5-iodo-4-pentenyl)-4-trifluoromethylbenzene. ^1H NMR (300 MHz, CDCl_3) δ 7.54 (d, $J = 8.0$ Hz, 2H), 7.27 (d, $J = 6.7$ Hz, 2H), 6.52 (dt, $J = 14.3, 7.1$ Hz, 1H), 6.03 (d, $J = 14.4$ Hz, 1H), 2.67 (t, $J = 7.7$ Hz, 2H), 2.09 (q, $J = 7.1$ Hz, 2H), 1.82 – 1.66 (m, 2H).

1-(Trifluoromethyl)-4-[(4E)-8-[(triisopropylsilyloxy]-4-octenyl]-benzene (14). To a flame dried round bottom flask under N_2 was added (allyloxy)triisopropylsilane (97 mg, 1.5 equiv, 0.45 mmol), 9-borabicyclo[3.3.1]nonane dimer (66 mg, 0.9 equiv, 27 mmol), and THF (4.0 mL, 1.0 M). The solution was left to stir for 4 hours at rt before being cooled to 0 °C. [1,1'-Bis(diphenylphosphino)ferrocene]dichloropalladium(II) (25 mg, 0.1 equiv, 0.03 mmol), NaOH (3.0 M, 0.4 mL, 4.0 equiv, 1.2 mmol) and (4E)-1-(5-iodo-4-pentenyl)-4-trifluoromethylbenzene (100 mg, 1.0 equiv, 0.3 mmol) were added to the flask. The reaction mixture was stirred at rt

overnight before it was quenched with NH_4Cl . The resulting mixture was extracted with DCM and the combined organic phases were dried with MgSO_4 and concentrated under vacuum. The crude product was purified with flash chromatography (SiO_2 : hexanes) to yield 20 mg (0.047 mmol, 16%) of 1-(Trifluoromethyl)-4-[(4*E*)-8-[(triisopropylsilyl)oxy]-4-octenyl]-benzene. ^1H NMR (500 MHz, CDCl_3) δ 7.52 (d, $J = 7.8$ Hz, 2H), 7.27 (d, $J = 7.8$ Hz, 2H), 5.44 (s, 2H), 3.68 (t, $J = 6.4$ Hz, 2H), 2.66 (t, $J = 7.7$ Hz, 2H), 2.15 – 1.94 (m, 4H), 1.82 – 1.54 (m, 4H), 1.16 – 0.96 (m, 21H). ^{13}C NMR (126 MHz, CDCl_3) δ 146.7, 130.8, 129.7, 128.7, 128.0 (q, $J = 32.3$ Hz), 125.2 (q, $J = 3.6$ Hz), 124.4 (q, $J = 273.3$ Hz), 62.8, 35.1, 32.9, 32.0, 31.0, 28.9, 18.0, 12.0. GC/MS calculated for $[\text{M}]^+$ 427.7, found 427.3. FTIR (neat, cm^{-1}): 3019 (w), 2942 (s), 2867 (s), 1670 (w), 1619 (m), 1464 (m), 1327 (s), 1165 (s), 1126 (s), 1068 (s).



Scheme 1.12. Synthesis of 1-(Trifluoromethyl)-4-[[trans-8-[(triisopropylsilyl)oxy]propyl]cyclopropylethyl]-benzene **18**

3-(4-Trifluoromethylphenyl)-1-ethanol (33). 4-(Trifluoromethyl)phenylacetic acid (2.0 g, 1.0 equiv, 10 mmol) was dissolved in tetrahydrofuran (23 mL, 0.4 M) and cooled to 0 °C. A borane tetrahydrofuran complex solution (1 M, 15 mL, 1.5 equiv, 15 mmol) was then added dropwise and

the reaction mixture was stirred at rt for 16 h. The reaction was quenched with water and extracted with DCM. The organic extract was dried with MgSO₄ and concentrated under vacuum to give 1.9 g (10 mmol, 100%) of 3-(4-trifluoromethylphenyl)-1-ethanol as a clear colorless oil. ¹H NMR (300 MHz, CDCl₃) δ 7.57 (d, *J* = 7.9 Hz, 2H), 7.35 (d, *J* = 7.9 Hz, 2H), 3.90 (t, *J* = 6.5 Hz, 2H), 2.93 (t, *J* = 6.4 Hz, 2H), 1.45 (s, 1H).

3-(4-Trifluoromethylphenyl)-1-ethyl trifluoromethanesulfonate (34). To a flame-dried reaction flask under N₂ was added 3-(4-trifluoromethylphenyl)-1-ethanol (570 mg, 1.0 equiv, 3.0 mmol), DCM (3.0 mL, 1.0 M), and 2,4-lutidine (0.38 mL, 1.1 equiv, 3.3 mmol). The reaction mixture was cooled to -78 °C and triflic anhydride (0.55 mL, 1.1 equiv, 3.3 mmol) was added dropwise. The mixture was left to stir at -78 °C for 30 min. Then, 20 mL of hexanes was added to the reaction flask and the mixture was poured onto a silica gel plug and the plug was washed with a 20:80 mixture of ethyl acetate:hexane. The filtrate was concentrated under vacuum to give 700 mg (2.2 mmol, 72%) of 3-(4-trifluoromethylphenyl)-1-ethyl trifluoromethanesulfonate as a clear colorless oil. ¹H NMR (300 MHz, CDCl₃) δ 7.62 (d, *J* = 8.0 Hz, 2H), 7.36 (d, *J* = 7.9 Hz, 2H), 4.72 (t, *J* = 6.7 Hz, 2H), 3.20 (t, *J* = 6.7 Hz, 2H).

1-[(4-Triethylsilyl)butyn-3-yl]-4-trifluoromethylbenzene (35). A solution of ethynyl trimethylsilane (0.36 mL, 1.2 equiv, 2.5 mmol) in THF (2.5 mL, 1.0 M) was cooled to -78 °C. *n*-BuLi (2.5 M, 0.83 mL, 1 equiv, 2.1 mmol) was added dropwise. The mixture was warmed to 0 °C and left to stir for 30 min. The reaction mixture was then cooled to -78 °C and 3-(4-trifluoromethylphenyl)-1-ethyl trifluoromethanesulfonate (700 mg, 1 equiv, 2.1 mmol) was added. The reaction was warmed to 0 °C and left to stir for 1 h. Then, water was added to quench the reaction and the product was extracted with DCM. The organic extract was dried with MgSO₄ and

concentrated under vacuum. The crude product was purified by flash chromatography (SiO₂: hexanes) to obtain 460 mg (1.7 mmol, 82%) of 1-[(4-triethylsilyl)butyn-3-yl]-4-trifluoromethylbenzene. ¹H NMR (300 MHz, CDCl₃) δ 7.55 (d, *J* = 8.1 Hz, 2H), 7.34 (d, *J* = 8.0 Hz, 2H), 2.88 (t, *J* = 7.3 Hz, 2H), 2.52 (t, *J* = 7.4 Hz, 2H), 0.13 (s, 9H).

[1-(3-Butynyl)-4-trifluoromethyl] benzene (36). In a round bottom flask, 1-[(4-triethylsilyl)butyn-3-yl]-4-trifluoromethylbenzene (430 mg, 1 equiv, 1.6 mmol) and tetra-*n*-butylammonium fluoride (1.0 M, 3.2 mL, 2 equiv, 3.2 mmol) were added. The mixture was stirred for 1 hour before water was added. The aqueous mixture was extracted with DCM. The organic extract was dried with MgSO₄ and concentrated under vacuum. The crude product was purified by flash chromatography (SiO₂: hexanes) to obtain 300 mg (1.5 mmol, 95%) of [1-(3-butynyl)-4-trifluoromethyl] benzene. ¹H NMR (300 MHz, CDCl₃) δ 7.56 (d, *J* = 8.0 Hz, 2H), 7.35 (d, *J* = 8.0 Hz, 2H), 2.90 (t, *J* = 7.3 Hz, 2H), 2.51 (td, *J* = 7.3, 2.6 Hz, 2H), 1.99 (t, *J* = 2.6 Hz, 1H).

(3E)-1-(4-Iodo-3-butenyl)-4-trifluoromethylbenzene (37). To a solution of 1-(3-butynyl)-4-trifluoromethylbenzene (240 mg, 1 equiv, 1.2 mmol) and Cp₂ZrCl₂ (390 mg, 1.1 equiv, 1.3 mmol) in THF (2.4 mL, 0.5 M) at rt was rapidly added a solution of LiAlH(Ot-Bu)₃ in THF (1 M, 1.3 mL, 1.1 equiv, 1.3 mmol). The resulting mixture was stirred at rt for 15 min. Then, a solution of I₂ (340 mg, 1.1 equiv, 1.3 mmol) in THF was added. After additional stirring at rt for 15 min, the reaction mixture was quenched with a solution of 1 N HCl and extracted with diethyl ether. The combined organic extract was washed successively with saturated Na₂SO₃, dried with MgSO₄ and concentrated under vacuum. The residue was subjected to flash chromatography (SiO₂: hexanes) to yield 360 mg (1.1 mmol, 92%) of (3E)-1-(4-iodo-3-butenyl)-4-trifluoromethylbenzene. ¹H

NMR (300 MHz, CDCl₃) δ 7.55 (d, J = 8.0 Hz, 2H), 7.27 (d, J = 8.0 Hz, 2H), 6.53 (dt, J = 14.3, 7.1 Hz, 1H), 6.05 (d, J = 14.4 Hz, 1H), 2.77 (t, J = 7.7 Hz, 2H), 2.38 (q, J = 7.6 Hz, 2H).

1-(Trifluoromethyl)-4-[(3E)-7-[(triisopropylsilyl)oxy]-3-octenyl]-benzene (38). To a flame dried round bottom flask under N₂ was added (allyloxy)triisopropylsilane (360 mg, 1.5 equiv, 1.7 mmol), 9-borabicyclo[3.3.1]nonane dimer (250 mg, 0.9 equiv, 1.0 mmol), and THF (4.0 ml, 1.0 M). The solution was left to stir for 4 hours at rt before being cooled to 0 °C. [1,1'-Bis(diphenylphosphino)ferrocene]dichloropalladium(II) (45 mg, 0.05 equiv, 0.06 mmol), NaOH (3.0 M, 1.4 mL, 4.0 equiv, 4.4 mmol) and (3E)-1-(4-iodo-3-butenyl)-4-trifluoromethylbenzene (360 mg, 1.0 equiv, 1.1 mmol) were added to the flask. The reaction mixture was stirred at rt overnight before it was quenched with NH₄Cl. The resulting mixture was extracted with DCM and the combined organic phases were dried with MgSO₄ and concentrated under vacuum. The crude product was purified with flash chromatography (SiO₂: hexanes) to yield 140 mg (0.33 mmol, 30%) of 1-(Trifluoromethyl)-4-[(3E)-7-[(triisopropylsilyl)oxy]-3-octenyl]-benzene. ¹H NMR (300 MHz, CDCl₃) δ 7.52 (d, J = 7.9 Hz, 2H), 7.27 (d, J = 8.4 Hz, 2H), 5.44 (s, 2H), 3.66 (t, J = 6.3 Hz, 2H), 2.72 (t, J = 7.5 Hz, 2H), 2.31 (s, 2H), 2.06 (s, 2H), 1.67 – 1.52 (m, 2H), 1.06 (s, 21H).

1-(Trifluoromethyl)-4-[[trans-8-[(triisopropylsilyl)oxy]propyl]cyclopropylethyl]-benzene (18). To a solution of diiodomethane (53 μ L, 2 equiv, 0.66 mmol) in DCM (0.66 mL, 0.5 M) being stirred at 0 °C under N₂ was added diethyl zinc (1 M, 0.66 mL, 2 equiv, 0.66 mmol), and the reaction was stirred for 10 min. A solution of 1-(Trifluoromethyl)-4-[(3E)-7-[(triisopropylsilyl)oxy]-3-octenyl]-benzene in DCM was added, and the reaction was stirred for 10 min before addition of a solution of TFA in DCM. The reaction was allowed to stir at 0 °C for 1 h before being

quenched by addition of cold saturated, aqueous NH_4Cl . The resulting mixture was extracted with DCM and the combined organic phases were dried with MgSO_4 and concentrated under vacuum. The crude product was purified with flash chromatography (SiO_2 : hexanes) to yield 72 mg (0.33 mmol, 51%) of 1-(trifluoromethyl)-4-[[trans-8-[(triisopropylsilyl)oxy]propyl]cyclopropylethyl]-benzene. ^1H NMR (300 MHz, CDCl_3) δ 7.52 (d, $J = 7.9$ Hz, 2H), 7.29 (d, $J = 7.9$ Hz, 2H), 3.69 (t, $J = 6.5$ Hz, 2H), 2.75 (t, $J = 7.6$ Hz, 2H), 1.58 (dq, $J = 14.7, 6.7$ Hz, 4H), 1.27 (t, $J = 9.6$ Hz, 3H), 1.19 – 0.91 (m, 20H), 0.59 – 0.33 (m, 2H), 0.32 – 0.13 (m, 2H). ^{13}C NMR (126 MHz, CDCl_3) δ 147.0, 128.9, 128.2 (q, $J = 32.2$ Hz), 125.3 (q, $J = 3.5$ Hz), 124.7 (q, $J = 283.7$ Hz), 63.4, 36.1, 36.1, 33.2, 30.6, 19.0, 18.6, 18.2, 12.2, 12.1. GC/MS calculated for $[\text{M}]^+$ 427.7, found 427.3. FTIR (neat, cm^{-1}): 3061 (w), 2942 (s), 2866 (s), 1619 (m), 1463 (m), 1327 (s), 1165 (s), 1126 (s).

***n*-Tridecane (20)** was purchased from Sigma-Aldrich and used as received.

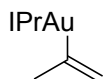
Dodecylbenzene (22) was synthesized according to literature procedure and its spectral data matches that reported.

1.4.4 *Synthesis and Characterization of Organogold Complexes*

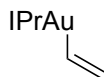
General Procedure of the Preparation of Organogold Complexes Through Transmetalation with a Grignard Reagent

To a dram vial under N_2 , diethyl ether and IPrAuCl (1 equiv) were added. The solution was cooled to -78 °C and grignard solution (1.1 equiv) was added dropwise. The mixture was warmed to room

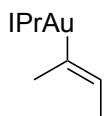
temperature and left to stir for 3 h. The reaction mixture was then filtered through a plug of magnesium sulfate and dried under vacuum to give a white powder.



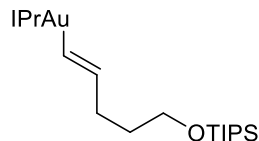
IPr(propenyl)Au(I) (1): Yield = 100%. ^1H NMR (300 MHz, CDCl_3) δ 7.46 (t, $J = 7.7$ Hz, 2H), 7.27 (d, $J = 5.1$ Hz, 4H), 7.10 (s, 2H), 5.27 (d, $J = 5.2$ Hz, 1H), 4.39 (d, $J = 5.2$ Hz, 1H), 2.62 (hept, $J = 2$ Hz), 1.66 (s, 1H), 1.36 (d, $J = 6.8$ Hz, 6H), 1.22 (d, $J = 6.9$ Hz, 6H). ^{13}C NMR (75 MHz, C_6D_6) δ 199.9, 175.5, 146.0, 135.2, 130.5, 124.2, 122.5, 119.5, 33.1, 29.1, 24.7, 24.0.



IPr(ethenyl)Au(I) (6): Has been previously characterized. Yield = 100%. ^1H NMR (500 MHz, C_6D_6) δ 7.47 (dd, $J = 20.7, 14.1$ Hz, 1H), 7.20 (t, $J = 7.7$ Hz, 2H), 7.06 (d, $J = 7.7$ Hz, 4H), 6.28 (s, 2H), 6.09 (dd, $J = 14.1, 6.0$ Hz, 1H), 5.52 (dd, $J = 20.7, 6.0$ Hz, 1H), 2.65 (sept, $J = 4$ Hz), 1.49 (d, $J = 6.8$ Hz, 12H), 1.09 (d, $J = 6.9$ Hz, 12H).



IPr(1-methyl-1-propenyl)Au(I) (26): Yield = 32%. ^1H NMR (500 MHz, C_6D_6) δ 7.23 (t, $J = 7.3$ Hz, 2H), 7.09 (d, $J = 7.4$ Hz, 4H), 6.45 (q, $J = 6.0$ Hz, 1H), 6.33 (s, 2H), 2.68 (sept, $J = 6.5$ Hz, 4H), 2.17 (s, 3H), 1.85 (d, $J = 5.8$ Hz, 3H), 1.50 (d, $J = 6.5$ Hz, 12H), 1.11 (d, $J = 6.6$ Hz, 12H). ^{13}C NMR (126 MHz, C_6D_6) δ 201.4, 165.6, 146.0, 135.2, 130.5, 128.3, 128.1, 127.9, 127.2, 124.1, 122.4, 122.4, 32.0, 29.1, 24.8, 24.0, 20.6.



IPr((*E*)-alkenyl)Au(I) (12)

In a N₂ filled glovebox, Schwartz's reagent (110 mg, 1.4 equiv, 0.44 mmol) and [(4-pentynyl)oxy]triisopropylsilane (64 mg, 1.0 equiv, 0.32 mmol) were weighed into a dram vial and allowed to stir for 30 min. IPrAuCl (200 mg, 1.0 equiv, 0.32 mmol) was added to the vial and the reaction mixture was left to stir for 3 h. Upon completion, the reaction was transferred to a 20 mL scintillation vial in the glovebox and concentrated in vacuo. The resulting residue was extracted using 2 mL of dry 1:1 pentane:diethyl ether. The solution was filtered through a pipette fitted with an oven-dried glass fiber filter to remove solid zirconocene dichloride. The filtered solution was then passed through a pipette containing basic alumina (c.a. 3 cm height) with additional pentane:diethyl ether solution (c.a. 4 mL) in order to remove any residual impurities. The filtrate was concentrated under vacuum to yield a 150 mg (0.19 mmol, 59%) of a white solid.⁵ ¹H NMR (500 MHz, C₆D₆) δ 7.17 (t, *J* = 7.7 Hz, 2H), 7.04 (d, *J* = 7.8 Hz, 4H), 6.82 (d, *J* = 18.3 Hz, 1H), 6.25 (s, *J* = 5.9 Hz, 2H), 5.69 (dt, *J* = 18.3, 6.0 Hz, 1H), 3.54 (t, *J* = 6.8 Hz, 2H), 2.62 (sept, *J* = 4H), 2.24 (q, *J* = 6.9 Hz, 2H), 1.64 (quin, *J* = 7.0 Hz, 2H), 1.46 (d, *J* = 6.8 Hz, 12H), 1.10 – 0.98 (m, 33H). ¹³C NMR (75 MHz, C₆D₆) δ 200.2, 155.6, 145.9, 144.1, 135., 130.5, 124.2, 122.5, 63.9, 35.3, 33.9, 29.1, 24.8, 24.0, 18.4, 12.5.

1.4.5 *Synthesis and Characterization of Alkyl Triflates*

General Procedure for the Preparation of Alkyl Triflates

A reaction flask was flame-dried under vacuum and allowed to cool under nitrogen. The flask was then charged with a stir bar, alcohol (1.0 equiv), DCM (1.0 M), and 2,6-lutidine (1.6 equiv). The mixture was cooled to -78 °C with a dry ice acetone bath. Triflic anhydride (1.2 equiv) was added dropwise to the cooled mixture with stirring. The reaction progress was monitored by TLC and when full conversion of the alcohol had occurred, the cold mixture was poured into hexanes (3x the reaction volume) in an Erlenmeyer flask. The mixture was immediately poured onto a silica plug and the plug was washed with a mixture of hexane and ethyl acetate that moves the product to R_f 0.5. The clean fractions from the silica gel plug were concentrated under reduced pressure and used without further purification.

3-[(Triisopropylsilyl)oxy]propyl trifluoromethanesulfonate (2): Yield = 78%. $^1\text{H NMR}$ (300 MHz, CDCl_3) δ 4.72 (t, $J = 6.2$ Hz, 2H), 3.83 (t, $J = 5.7$ Hz, 2H), 2.04 (quin, $J = 5.9$ Hz, 2H), 1.14 – 0.96 (m, 21H).

Dodecyl triflate (7): Yield = 48%. $^1\text{H NMR}$ (300 MHz, CDCl_3) δ 4.54 (t, $J = 6.5$ Hz, 2H), 1.95 – 1.74 (m, 2H), 1.45 – 1.18 (m, 18H), 0.88 (t, $J = 6.6$ Hz, 3H).

3-(4-Trifluoromethylphenyl)-1-propyl trifluoromethanesulfonate (13): Yield = 90%. $^1\text{H NMR}$ (500 MHz, CDCl_3) δ 7.58 (d, $J = 8.0$ Hz, 2H), 7.31 (d, $J = 7.9$ Hz, 2H), 4.54 (t, $J = 6.1$ Hz, 2H), 2.85 (t, $J = 7.6$ Hz, 1H), 2.18 (dt, $J = 13.2, 6.5$ Hz, 1H).

Chapter 2. NICKEL CATALYZED HYDROARYLATION OF ALKENES

2.1 INTRODUCTION

Unactivated alkenes are abundant and inexpensive feedstock materials. As such, their functionalization is an attractive and economical method to access more complex industrially or pharmaceutically relevant molecules. Catalytic hydroarylation of alkenes has been targeted as an attractive synthetic route to alkylarenes, a common structural motif in organic chemistry. Traditionally, hydroarylation is accomplished either via classical Friedel-Crafts reaction¹⁹ or through methods based on metal catalyzed C-H activation of arenes.²⁰ More recently, a third complementary strategy has been developed based on the reductive coupling of aryl halides and alkenes in the presence of a hydride donor. The key advance offered by reductive cross coupling relative to Friedel-Crafts and C-H activation methods is excellent site selectivity of the arene alkylation regardless of the substitution pattern of the starting arene.

The reductive cross coupling approach has been effectively used in several methods for the Markovnikov hydroarylation of alkenes. In 2016, Nakao et al. reported a Markovnikov hydroarylation of aryl alkenes using a dual palladium/copper catalyst system.²¹ The same year, Buchwald et al. reported an enantioselective version of the reaction using a similar approach.²² Markovnikov hydroarylation of alkenes has also been achieved by Herzon et al.²³ using transition metal hydrogen atom transfer (TM HAT) to initiate radical alkylation of arenes, and by Shenvi et al.²⁴ who used a distinct approach based on TM HAT coupled with nickel-catalyzed cross-coupling.

Anti-Markovnikov selectivity in the reductive cross coupling of aryl halides and alkenes is relatively rare. At the time we were developing this project, it had been achieved only in reactions of simple terminal alkenes (Fig. 2.1a). Buchwald et al. have shown that a dual palladium/copper catalyst system promotes coupling of unactivated alkenes with aryl halides to generate linear hydroarylation products.^{25, 26} Notably, the same catalyst system was previously shown to give Markovnikov selectivity in the hydroarylation of aryl alkenes.²² Recently, an alternative approach based on reductive Heck reaction has been successfully used by Engle et al.²⁷ and later Hu et al.²⁸ to access the same products. Relative to the excellent scope of the Engle's reaction of terminal alkyl alkenes, the scope of the Hu's reaction with aryl alkenes was limited.

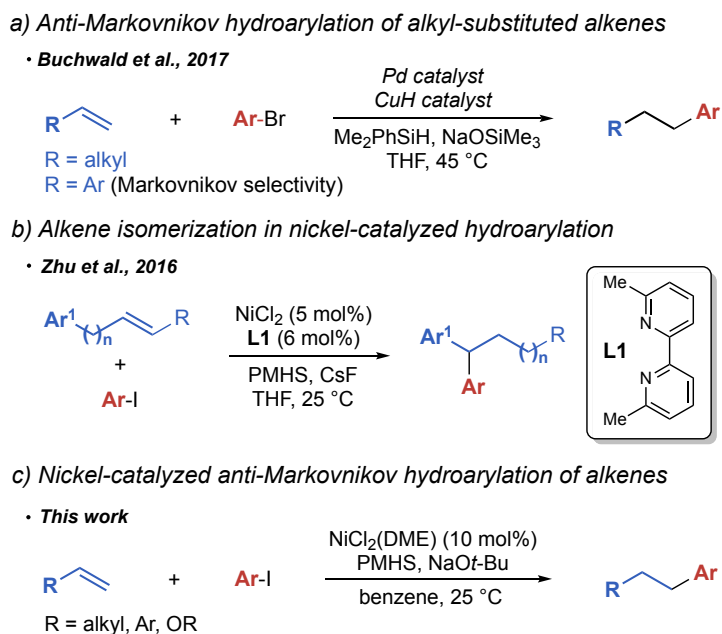


Figure 2.1. Reductive cross-coupling of alkenes with aryl halides

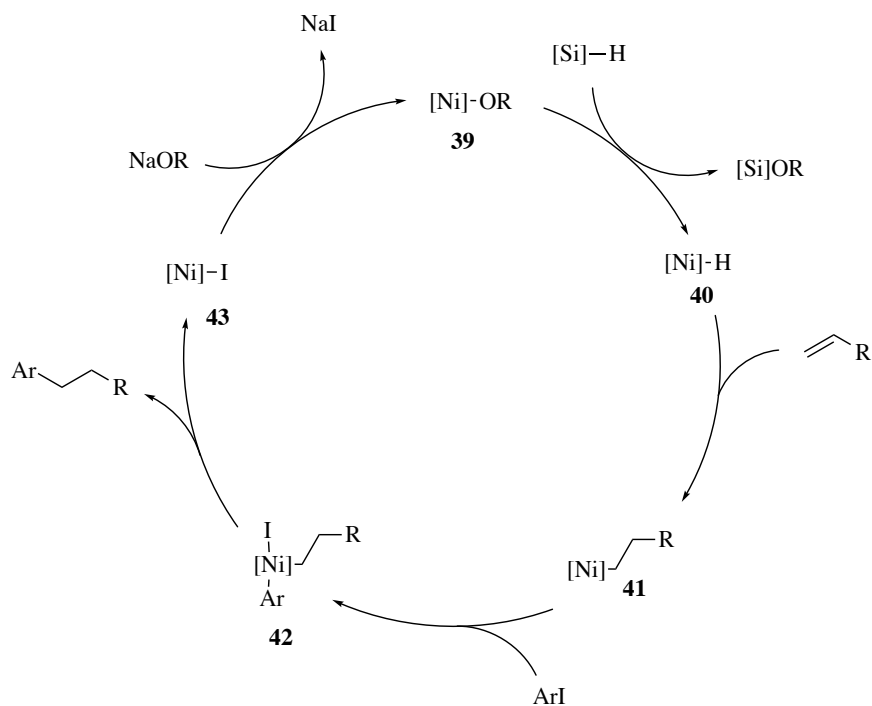
We were interested in developing a hydroarylation reaction that would complement existing methods and allow anti-Markovnikov hydroarylation of aryl alkenes and possibly other new substrate classes. Furthermore, we were hoping to achieve these transformations using a single metal complex as a catalyst. This catalyst would have to promote both the hydrometallation of alkenes and the subsequent cross coupling with aryl halides.

We focused on nickel complexes as particularly well suited for the task. Insertion of alkenes into nickel hydride complexes is well documented^{29, 30} and alkyl nickel complexes have

been implicated as intermediates in cross-coupling reactions with organohalides.³¹ Following an important precedent established by Liu et al.,³² the general feasibility of nickel-catalyzed hydroarylation was recently demonstrated by a reductive arylation reaction reported by Zhu et al. (Fig. 2.1b).^{33, 34} This transformation involved extensive isomerization of the alkene and the exclusive formation of 1,1-diaryl products regardless of the original position of the alkene relative to the arene.³⁵

In this work, we report the anti-Markovnikov hydroarylation of alkenes using a simple nickel catalyst. We are able to achieve this linear selectivity with a number of different substrate classes, including aryl alkenes, enol ethers and simple unactivated alkenes (Fig. 2.1c)³⁶

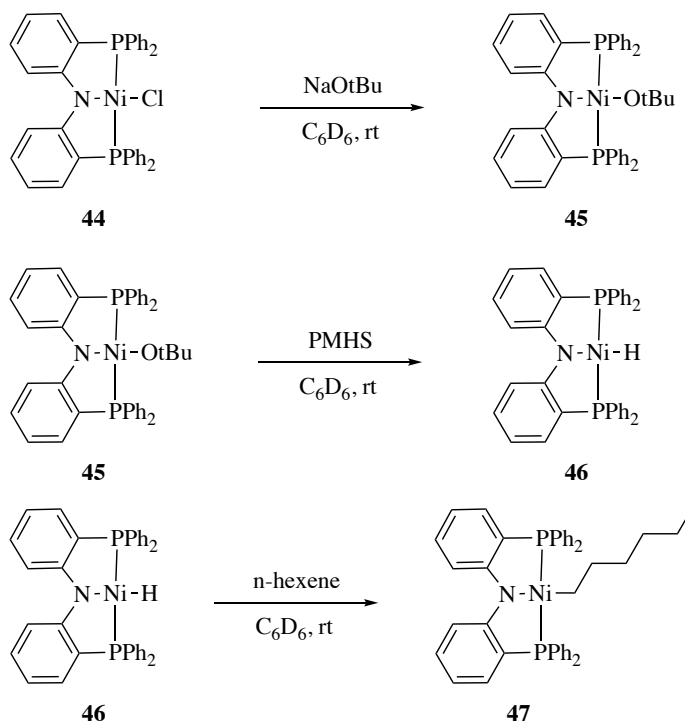
2.2 REACTION OPTIMIZATION



Scheme 2.1. Proposed mechanism for hydroarylation of alkenes

In 2008, Lee et al. reported a 1,2 insertion of 1-hexene into the Ni-H bond of an amido diphosphine supported Ni complex.³⁰ Inspired by this work, we envisioned developing a catalytic anti-Markovnikov method for the hydroarylation of alkenes where an insertion of an alkene into a nickel hydride complex would be a key elementary step. We hypothesized that a silane could be used to generate nickel hydride **40**, an alkene could insert into the Ni-H bond to form alkyl nickel complex **41** which could undergo an oxidative addition and reductive elimination sequence to generate the desired linear product, and a base could act as a turnover agent to regenerate catalyst **38** (Scheme 2.1).

To explore the feasibility of this catalytic cycle, we synthesized various Ni complexes supported by PNP pincer ligand $[N(o-C_6H_4PPh_2)_2]^-$ (Ph-PNP) and determined their competency in engaging in our proposed elementary steps (Scheme 2.2). Using ^{31}P NMR, we monitored the formation of nickel hydride **46** from nickel complex **45**. We found that adding silane to complex **44** was not enough to generate the hydride. The addition of

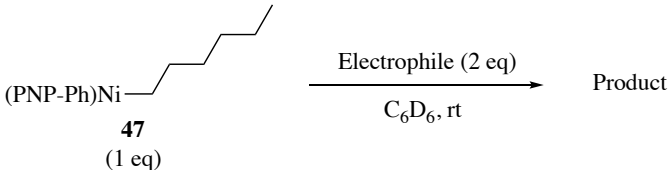


Scheme 2.2. Stoichiometric nickel reactions

NaOtBu to generate nickel alkoxide **45**, which occurred with complete conversion based on ^{31}P NMR, was a necessary first step. We tried several silanes and found that only polymethylhydrosiloxane (PMHS) gave complete conversion of nickel alkoxide **45** to nickel hydride **46**. Addition of 1-hexene to nickel hydride complex **46** quantitatively generated alkyl

nickel complex **47**. The isolated alkyl nickel complex **47** was found to react with a variety of electrophiles (Table 2.1.) and notably, two aryl electrophiles, iodobenzene and diphenyliodonium chloride, were competent reagents. We decided to focus on iodobenzene as an electrophile because, as a liquid, it is easier to use than diphenyliodonium chloride

Table 2.1. Stoichiometric reactions between alkyl Ni **47** and electrophiles

	
Electrophile	Yield(%) ^a
N-bromosuccinimide	26
Dodecyl triflate	2
1,2-Dibromotetrachloroethane	31
Iodobenzene	51
Diphenyliodonium chloride	59

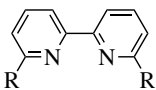
a) Yields were determined by GC after 24 h with 1, 3,5-trimethoxybenzene as a standard

Having found that our proposed elementary steps were viable, we next worked to develop a catalytic reaction with iodomethoxybenzene as the electrophile and styrene as the alkene. After screening various nickel complexes, we discovered that NiCl₂(DME) provides the hydroarylation product with excellent anti-Markovnikov selectivity (Table 2.2, entry 1). Essential for anti-Markovnikov selectivity and the overall success of the reaction was the absence of a ligand. A variety of ligands, including **L1** used by Zhu et al., resulted in no formation of the desired product (entries 2 and 3). For those ligands that did generate product, such as N-heterocyclic carbene ligand **IPr**, regioselectivity and yield were low (entry 4). Using different nickel sources, such as NiCl₂

(entry 5), resulted in lower yields. Interestingly, Ni(COD)₂, a Ni(0) source, proved to be competent in this reaction (entry 6).

Table 2.2. Nickel catalyzed hydroarylation reaction development^a

Entry	Variations from above	Yield (%) ^b	L:B ^c
1	none	89 (81)	55:1
2	L1 as a ligand	0	-
3	L2 as a ligand	0	-
4	IPr as a ligand	24	1.3: 1
5	NiCl ₂ instead of NiCl ₂ (dme)	44	15:1
6	Ni(COD) ₂ instead of NiCl ₂ (dme)	39	12:1
7	Toluene instead of benzene	80	48:1
8	1,4-dioxane	35	3:1
9	THF instead of benzene	8	2.5:1
10	(Me ₂ HSi) ₂ O instead of PMHS	57	29:1
11	LiO <i>t</i> -Bu instead of NaO <i>t</i> -Bu	30	7:1
12	KO <i>t</i> -Bu instead of NaO <i>t</i> -Bu	0	-



L1: R = Me
L2: R = H

a) Conditions: **48** (2 equiv), **49** (1 equiv), NaO*t*-Bu (4 equiv), PMHS (4 equiv).

b) Yields were determined by GC analysis of the crude reaction mixture using 1,3,5-trimethylbenzene as the internal standard. Number in parentheses is yield of isolated product

c) L:B is the ratio of the linear product to the branched product as determined by GC analysis of the crude reaction mixture

Aromatic solvents, such as benzene and toluene (entry 7), were essential for high yield of the hydroarylation product, while most other solvents were completely ineffective. Interestingly, ethereal solvents, such as 1,4-dioxane (entry 8) and THF (entry 9), provided significantly lower regioselectivity. PMHS was the best hydride source. Other silanes, including closely related $(\text{Me}_2\text{HSi})_2\text{O}$ (entry 10), provided lower yields and worse regioselectivity (see SI for details). Similarly, $\text{NaO}t\text{-Bu}$ was essential for the reaction and even the closely related Li and K analogs (entries 11 and 12) provided significantly inferior results. Exclusion of any component of this reaction resulted in no formation of product **50**.

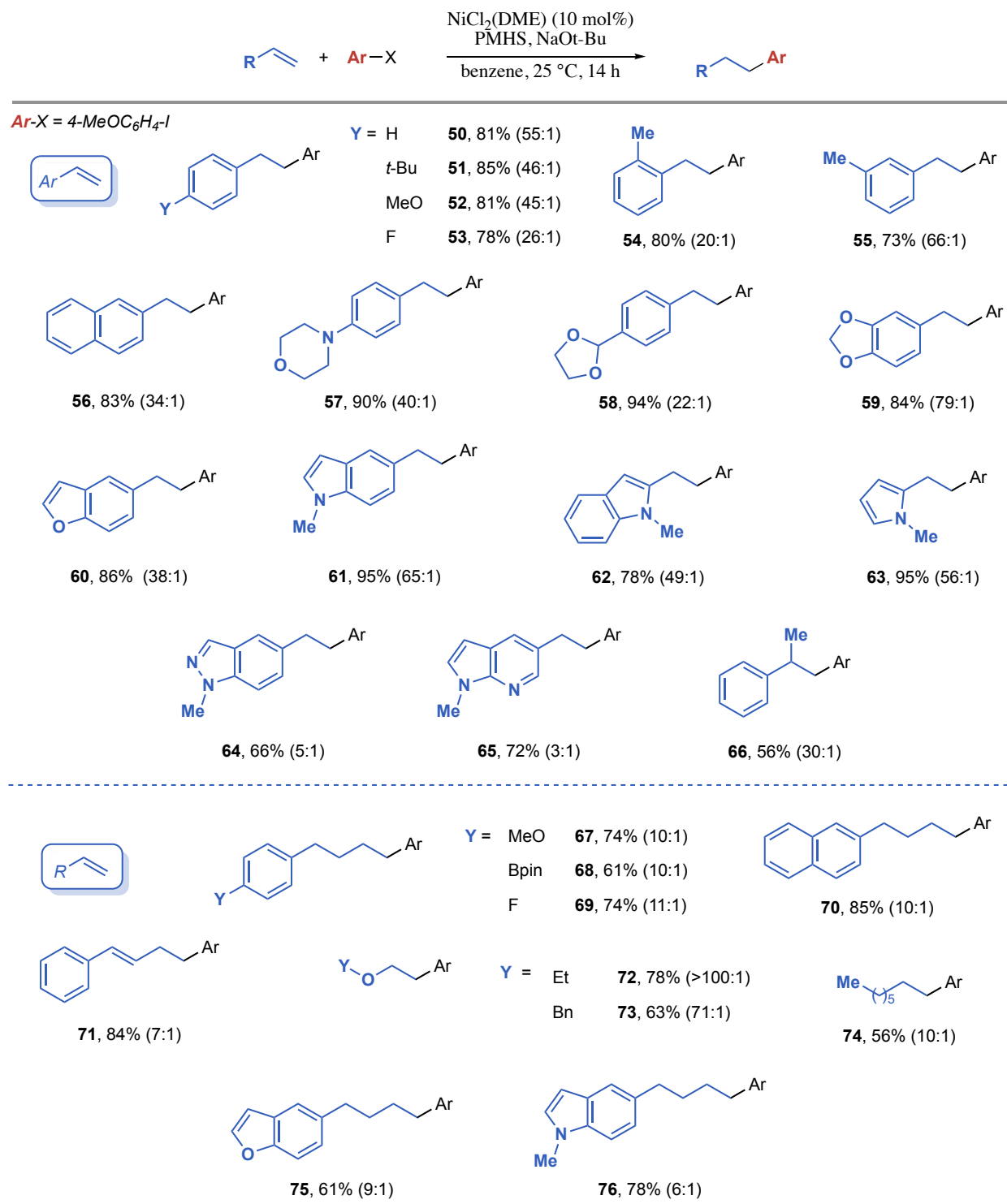
2.3 SUBSTRATE SCOPE

Hydroarylation could be achieved with a range of aryl- and alkyl-substituted alkenes (Table 2.3). With aryl alkenes, ortho, meta and para substitution is tolerated (compounds **54**, **55**, and **51**). Aryl alkenes containing both electron-donating and electron-withdrawing substituents are viable substrates (**52** and **53**). Good selectivities and yields were also obtained in hydroarylation of aryl alkenes containing a wide range of heteroarenes, including benzofuran (**60**), indole (**61** and **62**), pyrrole (**63**), benzopyrazole (**64**), and pyrrolopyridine (**65**). Finally, substitution on the α position of the alkene is also tolerated, as indicated by the formation of product **66** in the reaction with α -methylstyrene.

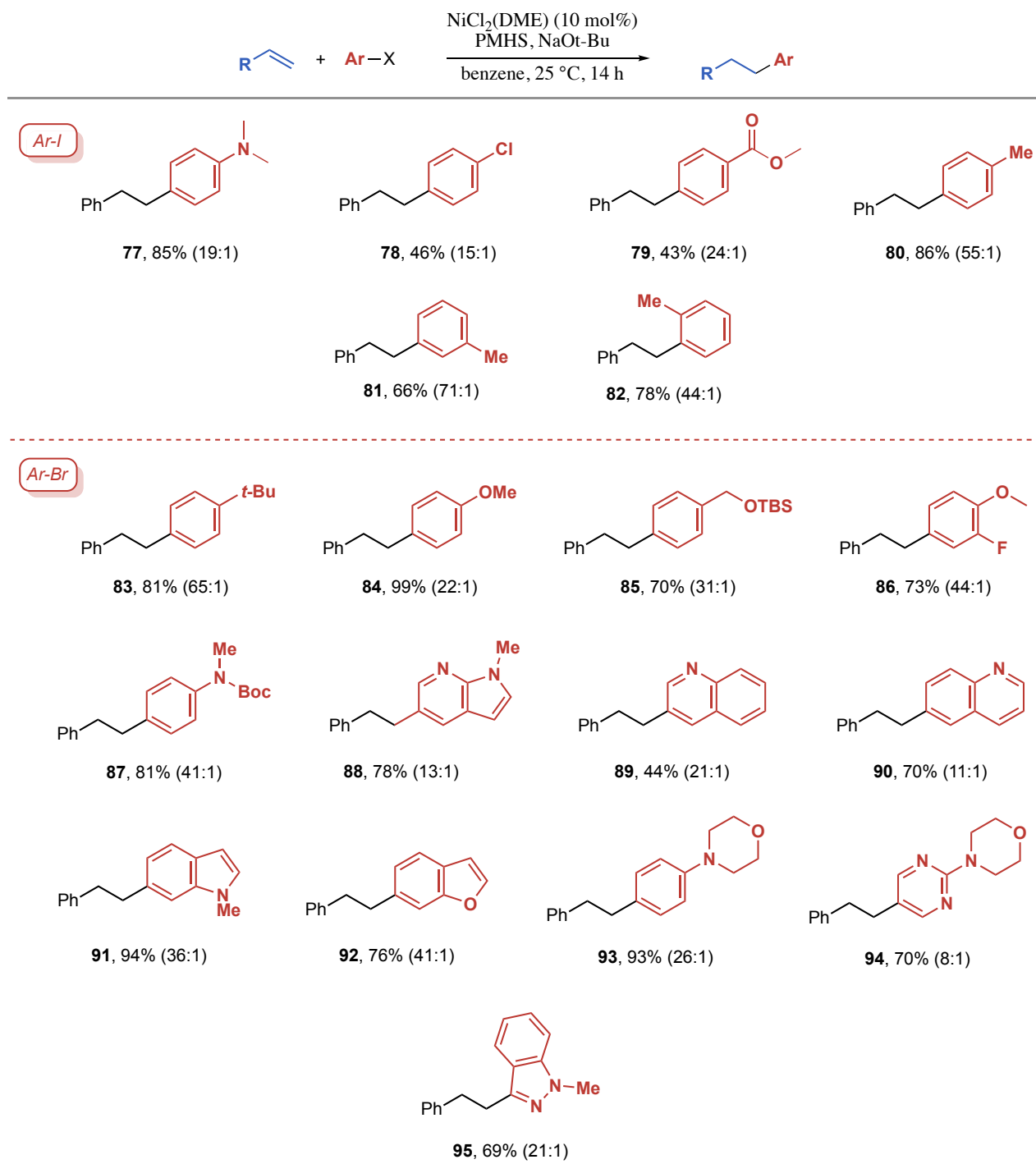
Nickel catalyzed hydroarylation of various other classes of alkenes was also examined. Unactivated terminal alkenes were suitable coupling partners (**67-70**, **74-76**), although the regioselectivity was somewhat lower. Surprisingly, a 1,3-diene substrate gave product **71** with high yield and good regioselectivity. Another unusual class of alkenes that were compatible with our reaction conditions is enol ethers. We were able to isolate the product of the reaction with

ethyl vinyl ether (**72**) in good yield (78%) while the benzyl protected enol ether provided the expected product **73** in 63% yield. To our knowledge, these are the only examples of anti-Markovnikov reductive cross coupling reactions with 1,3-dienes or enol ethers.

We have also explored the performance of various arene coupling partners, and both aryl iodides and aryl bromides are viable substrates (Table 2.4). The electronic properties of aryl electrophiles seem to play a significant role as electron-neutral and electron-rich aryl halides generally gave high yields (**77**, **84**, and **93**), while electron-poor aryl halides, though still competent, provided lower yields of the hydroarylation products (**78** and **79**). Again, we found that various heteroarenes are tolerated, including pyrrolopyridine (**88**), quinoline (**89** and **90**), indole (**91**), benzofuran (**92**), pyrimidine (**94**), and benzopyrazole (**95**).

Table 2.3. Alkene scope for nickel catalyzed hydroarylation^a

a) Conditions: Aryl halide (1 equiv), alkene (2 equiv), PMHS (4 equiv), NaOt-Bu (4 equiv). Yields of isolated products are reported. The ratios of linear to branched products were determined by GC analysis of the crude reaction mixture and are given in parenthesis.

Table 2.4. Aryl halide scope for nickel catalyzed hydroarylation^a

a) Conditions: Aryl halide (1 equiv), alkene (2 equiv), PMHS (4 equiv), NaOt-Bu (4 equiv). Yields of isolated products are reported. The ratios of linear to branched products were determined by GC analysis of the crude reaction mixture and are given in parenthesis.

2.4 MECHANISTIC STUDIES

A unique aspect of this new hydroarylation reaction is that the anti-Markovnikov selectivity obtained with a range of alkenes, including aryl alkenes and enol ethers. The observed selectivity is consistent with an addition of an aryl radical to the alkene, which would favor addition to the alkene terminus and formation of the more stable secondary alkyl radical (Fig. 2.2).

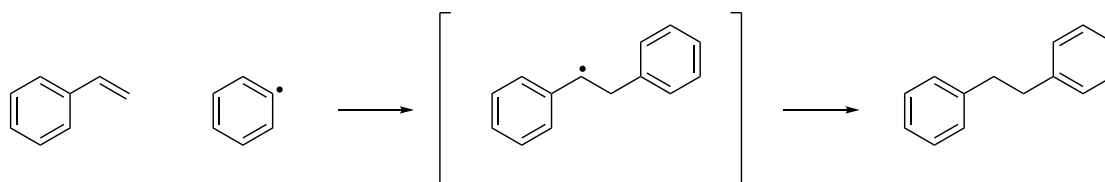


Figure 2.2. A possible radical mechanism

To test this mechanistic hypothesis, we synthesized three radical clocks and subjected them to the reaction conditions (Fig. 2.3). Unfortunately, the reactions between our radical clocks and 4-iodoanisole gave very low yields, making it very difficult to isolate and identify the products, and we were unable to make any conclusion on the basis of these reactions.

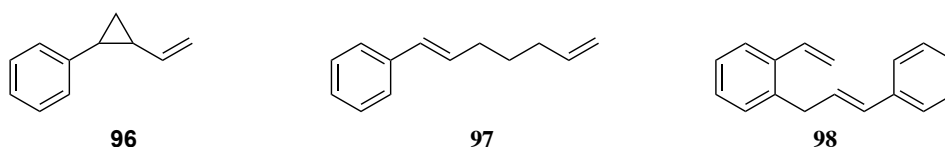
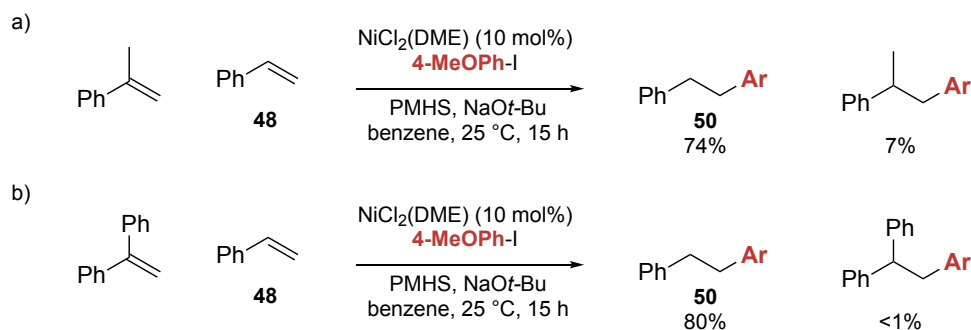


Figure 2.3. Radical traps

We also performed experiments in the presence of a radical trap. The presence of 10 mol% of TEMPO did lower the yield of the desired product and a full equivalent completely blocked its formation. However, in all cases, we observed only trace amounts (<5% yield) of the aryl-TEMPO adduct, suggesting that TEMPO likely interacts with another intermediate³⁷ and not with an aryl

radical. However, we cannot exclude the possibility that the Ar-TEMPO adduct reacts further under the reaction conditions.



Scheme 2.3. Competition experiments

In competition experiments (Scheme 2.3), we found that simple styrene reacts faster than α -methylstyrene and α -phenylstyrene, both of which should undergo radical addition faster than styrene. The results of these experiments are not consistent with a radical addition mechanism, leading us to explore other options.

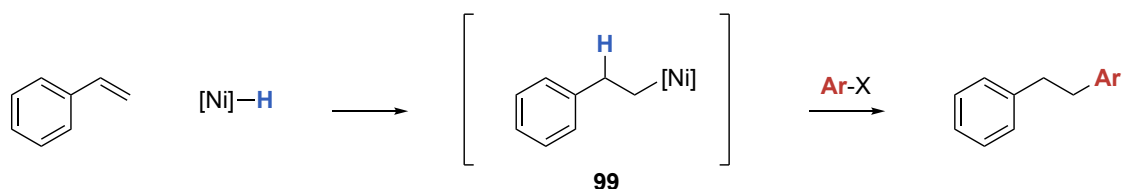
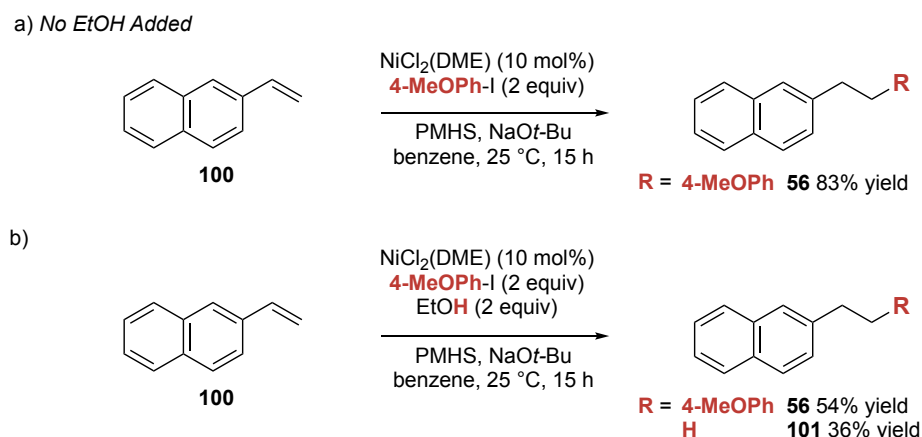


Figure 2.4. A possible hydrometallation mechanism

A mechanism involving hydrometallation followed by arylation of the alkyl nickel intermediate is another possible pathway (Fig. 2.4). This mechanism was proposed by Zhu et al. for their related hydroarylation reaction (Fig 2.1b). To explore whether an alkyl nickel complex, such as complex **99**, is an intermediate of our reaction, we decided to add EtOH to our reaction mixture. We would expect that such an addition could result in a competition reaction where alkyl

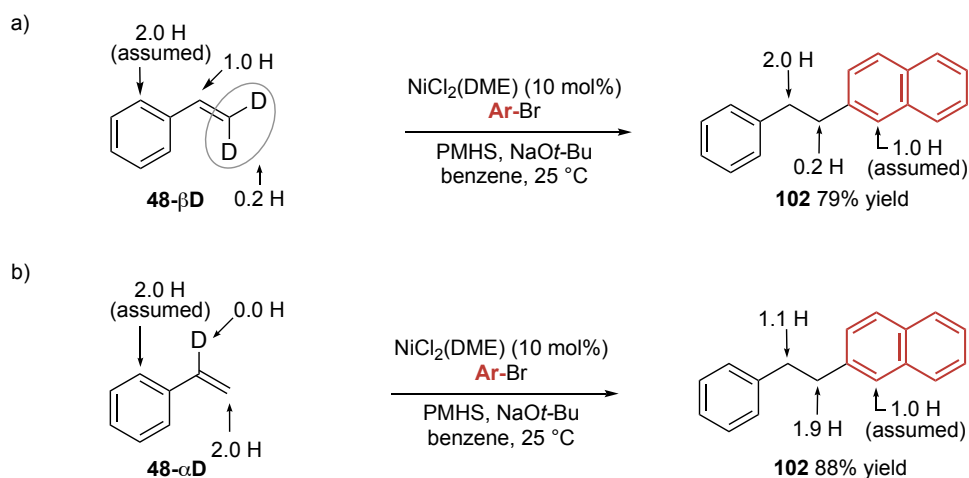
nickel species **99** could either react with EtOH to undergo protonation and produce an alkane product or react with aryl halide to produce the desired hydroarylation product. In the presence of 2 equiv of EtOH, the hydroarylation product is formed in a lower yield than in the absence of EtOH (54% vs 82%), while the alkane product **101** is formed in 36% yield (Scheme 2.4). This result is consistent with competitive protonation of an alkyl nickel intermediate. Based on these considerations, we propose that the hydroarylation reaction proceeds according to the mechanism shown previously in Scheme 2.1.



Scheme 2.4. Interception of alkyl nickel intermediate with EtOH

In the context of this mechanism, we were interested in the step that determines the regioselectivity of the reaction. In hydrofunctionalization reactions that proceed through hydrometallation, the product determining step varies depending on the reversibility of the hydrometallation step. When irreversible, hydrometallation is the regio-determining step. If hydrometallation is fast and reversible, there is a Curtin-Hammett scenario, and regioselectivity is determined by the relative rates of the irreversible reductive elimination at different sites and not by hydrometallation. Alkene insertion into nickel hydride complexes is often fast and

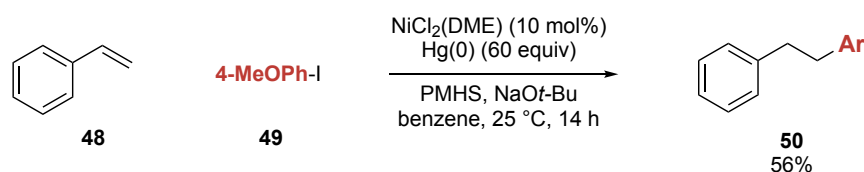
reversible,³⁸ as documented by Zhu et al. in their reductive arylation of alkenes.³³ Because the C-C bond-forming reductive elimination from nickel complexes tends to be exothermic,³⁹ the rates of reductive elimination are often based on the ground state stability of the alkyl metal intermediates. The result is that the reductive elimination from the most stable alkyl metal complex is favored.



Scheme 2.5. Deuterium scrambling experiments

To explore the reversibility of the hydrometallation step in the hydroarylation reaction, we used deuterium-labelled styrene substrates (Scheme 2.5). In the reaction with substrate **48- β D**, we observed no deuterium scrambling (Scheme 2.5a), while the reaction with **48- α D** resulted in minimal scrambling of the deuterium label (Scheme 2.5b). We did some further experiments to explore the source of the scrambling of the deuterium for substrate **48- α D**. We recovered and isolated **48- α D** from the reaction mixture and found that this substrate had undergone deuterium scrambling. We also found that with higher conversion, we saw greater scrambling in recovered **48- α D**. If the reaction with **48- α D** is stopped after 10 minutes, product **102** is isolated in 49% yield and no deuterium scrambling is observed in either the product or the recovered starting

material. These results suggest that the scrambling may be independent of the hydroarylation reaction. In the context of the reaction mechanism shown in Scheme 2.1, the two deuterium scrambling experiments point to hydrometallation being irreversible and the product determining step of the reaction. These results indicate that a strong kinetic preference for the formation of a homobenzylic alkyl nickel intermediate over the benzylic regioisomer is responsible for the regioselectivity of the hydroarylation.



Scheme 2.6. Addition of mercury to reaction mixture

The unusual selectivity in the hydrometallation of styrenes raises questions about the nature of the active catalyst. The absence of ligand in our hydroarylation reaction makes the formation of nanoparticles likely, and we observe an immediate formation of black particles upon the addition of the alkoxide to the reaction mixture. Mixtures of alkoxides and reducing reagents have previously been used to generate highly reactive nickel nanoparticle catalysts, and sodium alkoxide has been proposed to stabilize “ligandless” nickel catalysts.^{40,41} Furthermore, in the hydroarylation reaction, we observed a burst of initial activity (64% yield after 10 minutes), followed by a very slow reaction over the next 14 h when the maximum yield is achieved. Finally, we found that the addition of mercury significantly lowers the yield of the hydroarylation (56% vs 89% GC yields) (Scheme 2e).⁴² These observations are consistent with a heterogenous active catalyst.

2.5 CONCLUSION

We have developed a new method for the anti-Markovnikov hydroarylation of alkenes. The reaction involves reductive cross coupling of alkenes and aryl halides in the presence of a silane as a hydride donor. Anti-Markovnikov selectivity is obtained with a wide range of alkenes, including alkyl- and aryl-substituted alkenes, and enol ethers. Preliminary investigation of the reaction mechanism provides evidence for a mechanism that involves hydrometallation of the alkene, followed by coupling of the alkyl nickel intermediate with an aryl halide. The evidence points to highly selective hydrometallation of the alkene as the regioselectivity determining step of the reaction.

2.6 EXPERIMENTAL

2.6.1 *General Information*

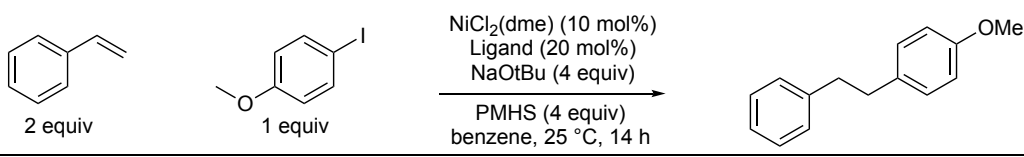
All reactions were performed under a nitrogen atmosphere with flame-dried or oven-dried (120 °C) glassware using standard Schlenk Technique, or in a glove box (Nexus II from Vacuum Atmospheres). Column chromatography was performed using a Biotage Iso-1SV flash purification system with silica gel from Agela Technologies Inc. (60Å, 40-60 µm, 230-400 mesh). Infrared (IR) spectra were recorded on a Perkin Elmer Spectrum RX I spectrometer. IR peak absorbencies are represented as follows: s = strong, m = medium, w = weak, br = broad. ¹H- and ¹³C-NMR spectra were recorded on a Bruker AV-300 or AV-500 spectrometer. ¹H NMR chemical shifts (δ) are reported in parts per million (ppm) downfield of TMS and are referenced relative to residual proteated solvent peak (CDCl₃ (7.26 ppm) or C₆D₆ (7.16 ppm)). ¹³C chemical shifts are reported in parts per million downfield of TMS and are referenced to the carbon resonance of the

solvent (CDCl_3 (δ 77.2 ppm)). Data are represented as follows: chemical shift, multiplicity (s = singlet, d = doublet, t = triplet, q = quartet, m = multiplet), integration, and coupling constants in Hertz (Hz). Mass spectra were collected on a JEOL HX-110 mass spectrometer. GC analysis was performed on a Shimadzu GC-2010 instrument with a flame ionization detector and a SHRXI-5MS column (15 m, 0.25 mm inner diameter, 0.25 μm film thickness). The following temperature program was used: 2 min @ 60 $^\circ\text{C}$, 13 $^\circ\text{C}/\text{min}$ to 160 $^\circ\text{C}$, 30 $^\circ\text{C}/\text{min}$ to 250 $^\circ\text{C}$, 5.5 min @ 250 $^\circ\text{C}$. Materials: Toluene, benzene, ether, DCM, and THF were degassed and dried by passing through columns of neutral alumina. All other solvents were used as received. Deuterated solvents were purchased from Cambridge Isotope Laboratories, Inc and were used as received. Commercial reagents were purchased from Sigma-Aldrich Co., VWR International, LLC., TCI Chemicals USA, or STREM Chemicals, Inc., and were used as received.

2.6.2 Reaction Development

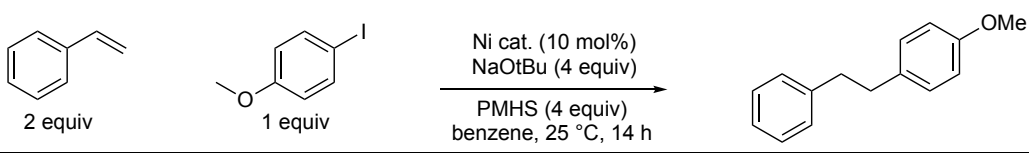
In a nitrogen filled glovebox, a dram vial was charged with a stir bar, and nickel catalyst (10 mol%) (Table S2). For the ligand screen (Table S1), ligand was added after addition of nickel. Stock solutions of silane, alkene, and the aryl halide were prepared in solvent (Table S3) at 0.5 mg/ μL concentrations. A stock solution of NaOt-Bu was prepared in solvent at a concentration of 0.1 mg/ μL . Silane (4.0 equiv) (Table S4), styrene (15.6 mg, 0.15 mmol, 3.0 equiv), and iodoanisole (11.7 mg, 0.05 mmol, 1.0 equiv) were added in quick succession. NaOt-Bu (19.1 mg, 0.20 mmol, 4.0 equiv) was added last. The reaction mixture was left to stir at room temperature for 14 h. Mesitylene (6.0 mg, 0.05 mmol, 1.0 equiv), an internal standard for GC analysis, was then added. A 30 μL aliquot was taken from the reaction mixture and filtered through a small plug of silica and rinsed with dichloromethane. Yields were determined by GC analysis using an internal standard.

Table 2.5. Ligand Screen



Entry	Ligand	Yield (%)	L:B
1	Phenanthroline	0	-
2	Bipyridine	0	-
3	6,6- Dimethyl-2,2-dipyridyl	0	-
4	PCy ₃	3	0.7: 1
5	Dppp	0	-
6	IPr	24	1.3:1

Table 2.6. Nickel Screen



Entry	Nickel Catalyst	Yield (%)	L:B
1	NiCl ₂	44	15:1
2	NiI ₂	15	13:1
3	Ni(COD) ₂	39	12:1

Table 2.7. Solvent Screen

Entry	Solvent	Yield (%)	L:B
1	Diethyl ether	38	14:1
2	Dioxane	35	3:1
3	THF	8	2.5:1
4	Pentane	61	75:1
5	Dichloromethane	9	24:1
6	Toluene	80	48:1

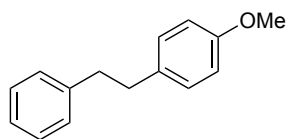
Table 2.8. Silane Screen

Entry	Silane	Yield (%)	L:B
1	TMDSO	57	29:1
2	Decamethylcyclopentasiloxane	34	24:1
3	Triethoxysilane	0	-
4	Triethylsilane	0	-
5	Diphenylsilane	33	13:1

2.6.3 General Procedure for the Hydroarylation of Alkenes

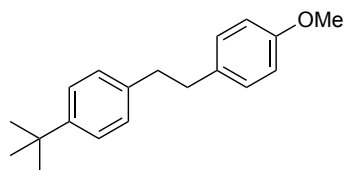
In a nitrogen filled glovebox, a dram vial was charged with a stir bar, and $\text{NiCl}_2(\text{dme})$ (5.5 mg, 0.025 mmol, 10 mol%). Solutions of PMHS, alkenes, and aryl halides were prepared in benzene at 0.5 mg/ μL concentrations. A stock solution of $\text{NaO}t\text{-Bu}$ was prepared in benzene at a concentration of 0.1 mg/ μL . PMHS (60.1 mg, 1.0 mmol, 4.0 equiv), alkene (0.50 mmol, 2.0 equiv), and aryl halide (0.25 mmol, 1.0 equiv) were added in quick succession. $\text{NaO}t\text{-Bu}$ (96.1 mg, 1.0 mmol, 4.0 equiv) was added last. The reaction mixture was stirred at room temperature for 14 h. The reaction was quenched by slowly adding methanol. After 30 mins, the resulting mixture was filtered through a silica plug. The resulting filtrate was then concentrated under reduced pressure and purified by silica gel column using a mixture of hexanes, toluene, and diethyl ether as the eluent. The regioselectivity of the hydroarylation was determined by GC analysis of the crude reaction mixture.

2.6.4 Characterization of Hydroarylation Products

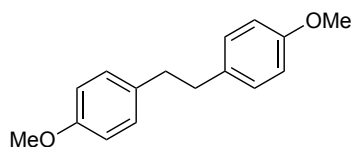


1-Methoxy-4-(2-phenylethyl)benzene (50) was isolated as a white solid (43.0 mg, 81%, 55:1 linear to branched ratio). ^1H NMR (300 MHz, CDCl_3) δ 7.34 – 7.27 (m, 2H), 7.24 – 7.19 (m, 3H), 7.13 (d, $J = 8.5$ Hz, 2H), 6.86 (d, $J = 8.5$ Hz, 2H), 3.82 (s, 3H), 2.91 (s, 4H). ^{13}C NMR (75 MHz, CDCl_3) δ 158.0, 142.0, 134.0, 129.5, 128.6, 128.4, 126.0, 113.9, 55.3, 38.3, 37.1. GCMS (EI)

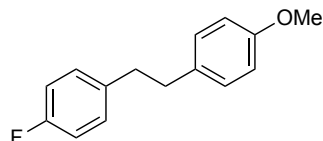
calculated for $[M]^+$ 212.12 found 212.10. FTIR (neat, cm^{-1}): 3062(m), 3028(m), 3002(m), 2934(s), 2857(m), 1612(m), 1511(s), 1246(s), 1037(m), 822(m).



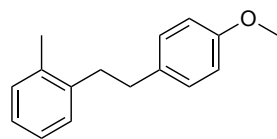
1-Tert-butyl-4-[2-(4-methoxyphenyl)ethyl]benzene (51) was isolated as a white solid (57.0 mg, 85%, 46:1 linear to branched ratio). ^1H NMR (500 MHz, CDCl_3) δ 7.36 (d, $J = 8.1$ Hz, 2H), 7.19 – 7.16 (m, 4H), 6.88 (d, $J = 8.5$ Hz, 1H), 3.83 (s, 3H), 2.90 (s, 4H), 1.36 (s, 9H). ^{13}C NMR (75 MHz, CDCl_3) δ 158.0, 148.8, 139.0, 134.3, 129.4, 128.2, 125.3, 113.9, 55.4, 37.8, 4.11, 34.5, 31.6. GCMS (EI) calculated for $[M]^+$ 268.18 found 268.10. FTIR (neat, cm^{-1}): 3051(m), 3021(m), 2991.4(m), 2961(s), 2902.0(m), 2866.5(m), 1612.1(m), 1512.6(s), 1245.7(s), 827.8(s).



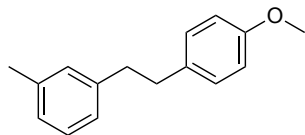
1-Methoxy-4-[2-(4-methoxyphenyl)ethyl]benzene (52) was isolated as a white solid (49.0 mg, 81%, 45:1 linear to branched ratio). ^1H NMR (300 MHz, CDCl_3) δ 7.11 (d, $J = 8.6$ Hz, 4H), 6.85 (d, $J = 8.6$ Hz, 4H), 3.81 (s, 6H), 2.86 (s, 4H). ^{13}C NMR (75 MHz, CDCl_3) δ 158.0, 134.1, 129.5, 113.9, 55.4, 37.4. GCMS (EI) calculated for $[M]^+$ 242.13 found 242.10. FTIR (neat, cm^{-1}): 3029(w), 3006(w), 2964(s), 2932(s), 2853(m), 1612(m), 1509(s), 1245(m), 1031(s), 832(s).



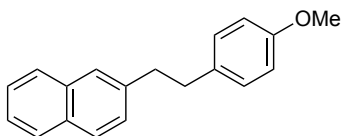
1-Fluoro-4-[2-(4-methoxyphenyl)ethyl]benzene (53) was isolated as a clear liquid (44.0 mg, 78%, 26:1 linear to branched ratio). ^1H NMR (300 MHz, CDCl_3) δ 7.19 – 7.02 (m, 4H), 6.99 – 6.93 (m, 2H), 6.83 (d, $J = 8.6$ Hz, 2H), 3.80 (s, 3H), 3.01 – 2.77 (m, 4H). ^{13}C NMR (75 MHz, CDCl_3) δ 161.5 (d, $J = 243.4$ Hz), 158.1, 137.6, 133.7, 130.0 (d, $J = 7.7$ Hz), 129.5, 115.1 (d, $J = 21.1$ Hz), 113.9, 55.4, 37.4, 37.2. GCMS (EI) calculated for $[\text{M}]^+$ 230.11 found 230.10. FTIR (neat, cm^{-1}): 3072(m), 3034(m), 3007(m), 2964(m), 2922(s), 2858(m), 1612(m), 1512(s), 1249(s), 1221(s) 1033(s), 835(s).



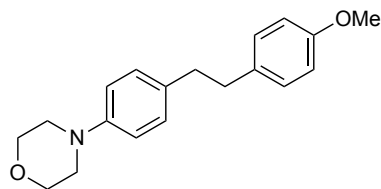
1-[2-(4-Methoxyphenyl)ethyl]-2-methylbenzene (54) was isolated as a clear liquid (45.1 mg, 80%, 20:1 linear to branched ratio). ^1H NMR (500 MHz, CDCl_3) δ 7.26 – 7.09 (m, 6H), 6.90 (d, $J = 6.7$ Hz, 2H), 3.83 (s, 3H), 2.95 – 2.86 (m, 4H), 2.36 (s, 3H). ^{13}C NMR (126 MHz, CDCl_3) δ 158.0, 140.2, 136.0, 134.2, 130.3, 129.4, 129.0, 126.2, 126.1, 113.9, 55.4, 36.0, 35.8, 19.4. GCMS (EI) calculated for $[\text{M}]^+$ 226.14 found 226.10. FTIR (neat, cm^{-1}): 3062(m), 3026(s), 2943(s), 2865(m), 1603(m), 1495(s), 1454(s), 1031(m), 754(s).



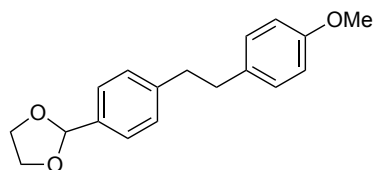
1-[2-(4-Methoxyphenyl)ethyl]-3-methylbenzene (55) was isolated as a clear liquid (41.2 mg, 73%, 66:1 linear to branched ratio). ^1H NMR (500 MHz, CDCl_3) δ 7.29 (dd, $J = 10.5, 4.6$ Hz, 1H), 7.24 – 7.16 (m, 2H), 7.16 – 7.02 (m, 3H), 6.98 – 6.85 (m, 2H), 3.88 (s, 3H), 2.97 (s, 4H), 2.45 (s, 3H). ^{13}C NMR (126 MHz, CDCl_3) δ 157.9, 141.9, 137.9, 134.1, 129.4, 129.4, 128.3, 126.7, 125.6, 113.8, 55.3, 38.3, 37.2, 21.5. GCMS (EI) calculated for $[\text{M}]^+$ 226.14 found 226.10. FTIR (neat, cm^{-1}): 3007(m), 2923(s), 2857(m), 2834(m), 1611(m), 1512(s), 1038(s), 822(m)



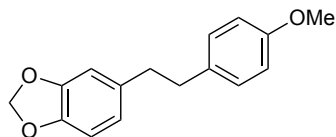
2-[2-(4-Methoxyphenyl)ethyl]-naphthalene (56) was isolated as a white solid (47.0 mg, 83%, 79:1 linear to branched ratio). ^1H NMR (500 MHz, CDCl_3) δ 7.83 (d, $J = 7.7$ Hz, 1H), 7.79 (d, $J = 8.3$ Hz, 2H), 7.63 (s, 1H), 7.51 – 7.41 (m, 2H), 7.35 (d, $J = 7.7$ Hz, 1H), 7.14 (d, $J = 8.4$ Hz, 2H), 6.85 (d, $J = 8.5$ Hz, 2H), 3.81 (s, 3H), 3.08 (dd, $J = 9.4, 6.4$ Hz, 2H), 2.98 (dd, $J = 9.5, 6.3$ Hz, 2H). ^{13}C NMR (75 MHz, CDCl_3) δ 158.1, 139.5, 134.0, 133.8, 132.2, 129.5, 128.0, 127.7, 127.6, 127.5, 126.6, 126.0, 125.3, 114.0, 55.4, 38.5, 37.0. GCMS (EI) calculated for $[\text{M}]^+$ 262.14 found 262.10. FTIR (neat, cm^{-1}): 3081(w), 3059(m), 3029(m), 2922(m), 2857(m), 1601(m), 1507(s), 1219(s), 830(s).



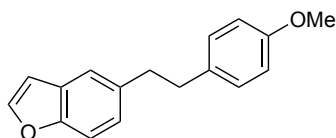
1-Methoxy-4-[2-(4-morpholinyl)ethyl]benzene (57) was isolated as a white solid (60.0 mg, 90%, 40:1 linear to branched ratio). ^1H NMR (500 MHz, CDCl_3) δ 7.10 (d, $J = 8.3$ Hz, 4H), 6.87 – 6.83 (m, 4H), 3.95 – 3.84 (m, 4H), 3.80 (s, $J = 7.6$ Hz, 3H), 3.19 – 3.09 (m, 4H), 2.84 (s, $J = 16.8$ Hz, 4H). ^{13}C NMR (126 MHz, CDCl_3) δ 158.00, 149.69, 134.24, 133.75, 129.51, 129.32, 116.04, 113.91, 67.15, 55.41, 49.93, 37.39, 37.31. GCMS (EI) calculated for $[\text{M}]^+$ 297.40 found 297.10. FTIR (neat, cm^{-1}): 3007 (w), 2950 (m), 2918 (m), 2857 (m), 1610 (m), 1513 (s), 1303 (m), 1261 (m), 1244 (m), 1031 (m), 923 (m).



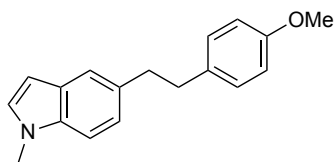
2-[4-[2-(4-Methoxyphenyl)ethyl]phenyl]-1,3-dioxolane (58) was isolated as a white solid (67.0 mg, 94%, 22:1 linear to branched ratio). ^1H NMR (300 MHz, CDCl_3) δ 7.42 (d, $J = 8.0$ Hz, 2H), 7.21 (d, $J = 8.0$ Hz, 2H), 7.11 (d, $J = 8.5$ Hz, 2H), 6.84 (d, $J = 8.5$ Hz, 2H), 5.81 (s, 1H), 4.19 – 3.99 (m, 4H), 3.80 (s, 3H), 3.05 – 2.75 (m, 4H). ^{13}C NMR (75 MHz, CDCl_3) δ 158.0, 143.1, 135.6, 133.8, 129.4, 128.6, 126.6, 113.9, 103.9, 65.4, 55.4, 38.0, 37.0. GCMS (EI) calculated for $[\text{M}]^+$ 284.14 found 284.10. FTIR (neat, cm^{-1}): 3021(w), 2962(m), 2920(m), 2850(m), 1609(m), 1512(s), 1245(s), 1037(s), 827(s).



5-[2-(4-Methoxyphenyl)ethyl]-1,3-benzodioxole (59) was isolated as a white solid (54.0 mg, 84%, 79:1 linear to branched ratio). ^1H NMR (300 MHz, CDCl_3) δ 7.08 (d, $J = 8.5$ Hz, 2H), 6.82 (d, $J = 8.5$ Hz, 2H), 6.77 – 6.53 (m, 3H), 5.92 (s, 2H), 3.79 (s, 3H), 2.81 (s, 4H). ^{13}C NMR (126 MHz, CDCl_3) δ 158.0, 147.6, 145.8, 135.9, 133.9, 129.5, 121.4, 113.9, 109.2, 108.2, 100.9, 55.4, 38.0, 37.4. GCMS (EI) calculated for $[\text{M}]^+$ 262.14 found 262.10. FTIR (neat, cm^{-1}): 3029(w), 2991(m), 2930(s), 2857(m), 1611(m), 1512(s), 1489(s), 1245(s), 1038(s), 810(m).

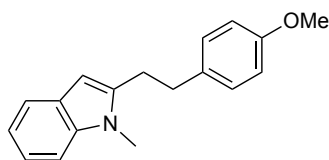


5-[2-(4-Methoxyphenyl)ethyl]benzofuran (60) was isolated as a white solid (54.0 mg, 86%, 38:1 linear to branched ratio). ^1H NMR (300 MHz, CDCl_3) δ 7.60 (d, $J = 2.2$ Hz, 1H), 7.47 – 7.35 (m, 2H), 7.14 – 7.10 (m, 3H), 6.88 – 6.78 (m, 2H), 6.72 (d, $J = 2.1$, 1H), 3.07 – 2.86 (m, 4H). ^{13}C NMR (75 MHz, CDCl_3) δ 153.81, 145.23, 136.53, 134.12, 129.55, 125.18, 120.71, 113.94, 111.16, 106.59, 55.42, 38.27, 37.83. GCMS (EI) calculated for $[\text{M}]^+$ 252.31 found 252.10. FTIR (neat, cm^{-1}): 2965 (w), 2929 (m), 2915 (m), 2849 (m), 1611 (m), 1514 (m), 1102 (m), 1032 (s), 824 (s).

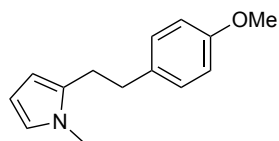


1-Methyl-5-[2-(4-methoxyphenyl)ethyl]-1H-indole (61) was isolated as a pale orange solid (63.0 mg, 95%, 65:1 linear to branched ratio). ^1H NMR (300 MHz, CDCl_3) δ 7.55 (d, $J = 7.7$ Hz, 1H),

7.31 – 7.22 (m, 1H), 7.22 – 7.03 (m, 4H), 6.85 (d, $J = 8.6$ Hz, 2H), 6.31 (s, 1H), 3.80 (s, 3H), 3.60 (s, 3H), 3.01 (s, 4H). ^{13}C NMR (126 MHz, CDCl_3) δ 158.23, 140.78, 137.46, 133.57, 129.48, 128.03, 120.79, 120.00, 119.42, 114.07, 108.94, 99.00, 55.44, 34.45, 29.51, 29.36. GCMS (EI) calculated for $[\text{M}]^+$ 265.36 found 265.10. FTIR (neat, cm^{-1}): 3011 (w), 2962 (m), 2933 (m), 28554 (m), 1608 (m), 1512 (s), 1493 (m), 1245 (s), 1031 (m), 825 (m).

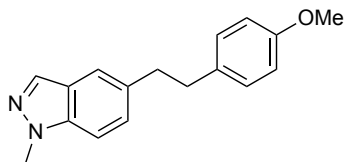


1-Methyl-2-[2-(4-methoxyphenyl)ethyl]-1H-indole (62) was isolated as a pale orange solid (52.0 mg, 78%, 49:1 linear to branched ratio). ^1H NMR (500 MHz, CDCl_3) δ 7.49 (s, 1H), 7.28 (d, $J = 8.3$ Hz, 1H), 7.18 (d, $J = 8.2$ Hz, 2H), 7.12 (d, $J = 8.3$ Hz, 1H), 7.06 (d, $J = 2.7$ Hz, 1H), 6.88 (d, $J = 8.2$ Hz, 2H), 6.47 (d, $J = 2.6$ Hz, 1H), 3.83 (s, 3H), 3.80 (s, 3H), 3.08 – 2.92 (m, 4H). ^{13}C NMR (75 MHz, CDCl_3) δ 157.92, 135.60, 134.62, 132.93, 129.53, 129.03, 128.84, 122.71, 120.20, 113.88, 109.10, 100.67, 55.39, 38.51, 38.11, 32.93. GCMS (EI) calculated for $[\text{M}]^+$ 265.36 found 265.10. FTIR (neat, cm^{-1}): 3051 (w), 2967 (m), 2933 (m), 2873 (m), 1611 (m), 1469 (s), 1370 (m), 1316 (m), 1232 (m), 1128 (m), 745 (s).

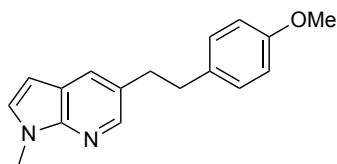


1-Methyl-2-[2-(4-methoxyphenyl)ethyl]-1H-pyrrole (63) was isolated as a pale orange solid (51.0 mg, 95%, 56:1 linear to branched ratio). ^1H NMR (300 MHz, CDCl_3) δ 7.15 (d, $J = 8.6$ Hz, 2H), 6.94 – 6.80 (m, 2H), 6.63 – 6.50 (m, 1H), 6.16 – 6.05 (m, 1H), 6.01 – 5.92 (m, 1H), 3.82 (s,

3H), 3.49 (s, 3H), 2.99 – 2.72 (m, 4H). ^{13}C NMR (75 MHz, CDCl_3) δ 158.19, 134.07, 133.09, 129.44, 121.23, 114.05, 106.78, 105.76, 55.45, 34.83, 33.59, 28.91. GCMS (EI) calculated for $[\text{M}]^+$ 215.30 found 215.10. FTIR (neat, cm^{-1}): 3099 (w), 3029 (m), 2994 (m), 2933 (w), 2834 (m), 1611 (m), 1513 (s), 1494 (m), 1301 (m), 1246 (m), 1171 (m), 1036 (m), 822 (m).

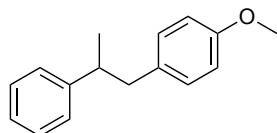


1-Methyl-5-[2-(4-methoxyphenyl)ethyl]-1H-indazole (64) was isolated as a pale orange solid (44.0 mg, 66%, 5:1 linear to branched ratio). ^1H NMR (300 MHz, CDCl_3) δ 7.80 (d, $J = 5.3$ Hz, 1H), 7.60 (dd, $J = 13.9, 8.9$ Hz, 1H), 7.40 (d, $J = 27.6$ Hz, 1H), 7.24 – 7.02 (m, 3H), 6.82 (dd, $J = 8.7, 3.2$ Hz, 2H), 4.20 (s, 3H), 3.79 (s, 3H), 3.11 – 2.74 (m, 4H). ^{13}C NMR (75 MHz, CDCl_3) δ 158.05, 135.19, 134.14, 129.55, 128.77, 128.26, 123.45, 123.15, 118.09, 117.18, 113.95, 55.43, 40.34, 38.52, 37.17. GCMS (EI) calculated for $[\text{M}]^+$ 266.34 found 266.10. FTIR (neat, cm^{-1}): 2962 (m), 2914 (m), 2849 (m), 1611 (m), 1511 (m), 1246 (m), 1177 (m), 1033 (m), 821 (m).

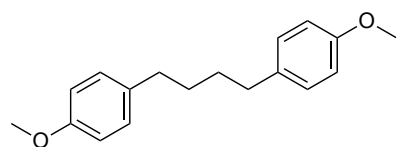


1-Methyl-5-[2-(4-methoxyphenyl)ethyl]-1H-pyrrolo[2,3-*b*]pyridine-5-yl (65) was isolated as a pale orange solid (48.0 mg, 72%, 3:1 linear to branched ratio). ^1H NMR (500 MHz, CDCl_3) δ 8.15 (s, 1H), 7.67 (s, 1H), 7.14 (d, $J = 3.2$ Hz, 1H), 7.09 (d, $J = 8.2$ Hz, 2H), 6.82 (d, $J = 8.2$ Hz, 2H), 6.37 (d, $J = 3.3$ Hz, 1H), 3.87 (s, 3H), 3.79 (s, 3H), 3.06 – 2.85 (m, 4H). ^{13}C NMR (75 MHz,

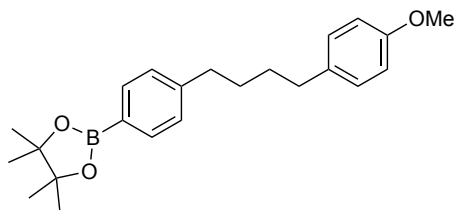
CDCl₃) δ 158.13, 147.02, 143.72, 133.81, 129.59, 129.33, 128.76, 128.53, 120.59, 114.03, 99.04, 55.44, 37.85, 35.56, 31.44. GCMS (EI) calculated for [M]⁺ 266.34 found 266.10. FTIR (neat, cm⁻¹): 3005 (w), 2930, (m), 2855 (m), 1611 (m), 1512 (m), 1402 (m), 1300 (w), 1245 (m), 1177 (m), 1035 (m), 822 (w).



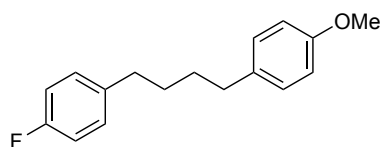
1-Methoxy-4-(2-phenylpropyl)benzene (66) was isolated as a white solid (31.6 mg, 56%, 30:1 linear to branched). ¹H NMR (500 MHz, CDCl₃) δ 7.36 (t, *J* = 7.6 Hz, 2H), 7.31 – 7.20 (m, 3H), 7.07 (d, *J* = 8.4 Hz, 2H), 6.86 (d, *J* = 8.5 Hz, 2H), 3.82 (s, 3H), 3.04 (qt, *J* = 14.3, 7.0 Hz, 1H), 2.97 (dd, *J* = 13.4, 6.5 Hz, 1H), 2.80 (dd, *J* = 13.4, 8.1 Hz, 1H), 1.32 (d, *J* = 6.8 Hz, 3H). ¹³C NMR (126 MHz, CDCl₃) δ 157.9, 147.1, 133.0, 130.1, 128.4, 127.2, 126.1, 113.6, 55.2, 44.2, 42.1, 21.2. GCMS (EI) calculated for [M]⁺ 226.14 found 226.10. FTIR (neat, cm⁻¹): 3061(m), 3028(m), 2959(s), 2928(s), 2834(m), 1612(m), 1512(s), 1247(s), 1178(m), 1037(m), 818(m).



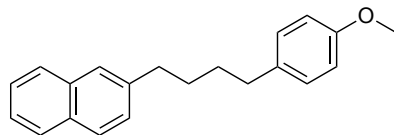
1,4-Bis(4-methoxyphenyl)butane (67) was isolated as a white solid (51.1 mg, 74%, 10:1 linear to branched ratio). ¹H NMR (500 MHz, CDCl₃) δ 7.14 (d, *J* = 7.6 Hz, 4H), 6.88 (d, *J* = 7.5 Hz, 4H), 3.83 (s, 6H), 2.63 (s, 4H), 1.68 (s, 4H). ¹³C NMR (126 MHz, CDCl₃) δ 157.8, 134.8, 129.4, 113.8, 55.3, 35.0, 31.4. GCMS (EI) calculated for [M]⁺ 270.16 found 270.1. FTIR (neat, cm⁻¹): 3056(w), 3004(m), 2932(s), 2853(m), 2834(m), 1613(m), 1513(s), 1246(s), 1035(s), 816(s).



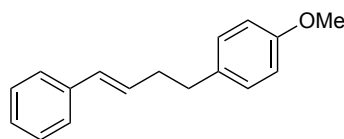
2-[4-(4-(4-Methoxyphenyl)butyl)phenyl]-4,4,5,5-tetramethyl-1,3,2-dioxaborolane (68) was isolated as clear liquid (56.0 mg, 61%, 10:1 linear to branched ratio). ^1H NMR (300 MHz, CDCl_3) δ 7.73 (d, $J = 7.5$ Hz, 2H), 7.19 (d, $J = 7.6$ Hz, 2H), 7.08 (d, $J = 8.2$ Hz, 2H), 6.82 (d, $J = 8.3$ Hz, 2H), 3.79 (s, 3H), 2.65-2.55 (m, 4H), 1.84 – 1.48 (m, 4H), 1.34 (s, $J = 23.0$ Hz, 12H). ^{13}C NMR (75 MHz, CDCl_3) δ 157.9, 146.2, 135.0, 134.8, 129.4, 128.0, 113.9, 83.8, 55.4, 36.2, 35.0, 31.4, 31.0, 25.0. GCMS (EI) calculated for $[\text{M}]^+$ 366.24 found 366.20. FTIR (neat, cm^{-1}): 3040(m), 3004(m), 2958(s), 2929(s), 2858(s), 2104(m), 1601(m), 1490(s), 1221(s), 823(s).



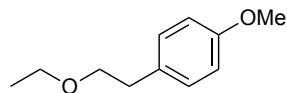
1-Fluoro-4-[4-(4-methoxyphenyl)butyl]benzene (69) was isolated as a clear liquid (48.0 mg, 74%, 11:1 linear to branched ratio). ^1H NMR (300 MHz, CDCl_3) δ 7.17 – 7.01 (m, 4H), 7.01 – 6.87 (m, 2H), 6.82 (d, $J = 8.5$ Hz, 2H), 3.79 (s, 3H), 2.59 (d, $J = 6.8$ Hz, 4H), 1.80 – 1.48 (m, 4H). ^{13}C NMR (126 MHz, CDCl_3) δ 160.3, 160.1 (d, $J = 559.1$ Hz), 138.3, 134.7, 129.8 (d, $J = 7.6$ Hz), 129.4, 115.1 (d, $J = 21.0$ Hz), 113.8, 55.4, 35.1, 34.97, 31.33, 31.25. GCMS (EI) calculated for $[\text{M}]^+$ 258.14 found 258.10. FTIR (neat, cm^{-1}): 3036(m), 2999(m), 2932(s), 2857(m), 1612 (m), 1510(s), 1246(m), 1220(m), 1036(m), 822(m).



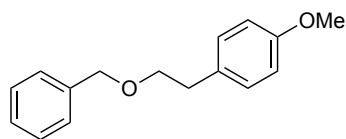
2-[4-(4-Methoxyphenyl)butyl]naphthalene (70) was isolated as a white solid (61.5 mg, 85%, 10:1 linear to branched ratio). ^1H NMR (500 MHz, CDCl_3) δ 7.82 (d, $J = 7.8$ Hz, 1H), 7.78 (d, $J = 7.8$ Hz, 2H), 7.61 (s, 1H), 7.49 – 7.38 (m, 2H), 7.34 (d, $J = 8.3$ Hz, 1H), 7.10 (d, $J = 7.7$ Hz, 2H), 6.84 (d, $J = 7.8$ Hz, 2H), 3.80 (s, 3H), 2.81 (t, $J = 7.1$ Hz, 2H), 2.62 (t, $J = 7.2$ Hz, 2H), 1.85 – 1.61 (m, 4H). ^{13}C NMR (75 MHz, CDCl_3) δ 157.9, 140.3, 134.8, 133.8, 132.2, 129.4, 127.9, 127.7, 127.6, 126.5, 126.0, 125.2, 113.9, 55.4, 36.1, 35.1, 31.4, 31.0. GCMS (EI) calculated for $[\text{M}]^+$ 290.17 found 290.10. FTIR (neat, cm^{-1}): 3052(m), 2929(s), 2854(m), 1612(m), 1512(s), 1247(s), 1037(m), 817(m).



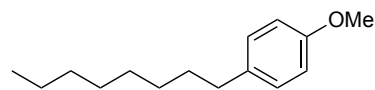
1-Methoxy-4-(4-phenylbut-3-en-1-yl)benzene (71) was isolated as a clear liquid (50.0 mg, 84%, 7:1 linear to branched ratio). ^1H NMR (300 MHz, CDCl_3) δ 7.43 – 7.25 (m, 4H), 7.25 – 7.07 (m, 3H), 6.92 – 6.78 (m, 2H), 6.43 (d, $J = 15.9$ Hz, 1H), 6.27 (dt, $J = 15.8, 6.6$ Hz, 1H), 3.82 (s, 3H), 2.76 (t, $J = 7.7$ Hz, 2H), 2.55 – 2.48 (m, 2H). ^{13}C NMR (126 MHz, CDCl_3) δ 158.0, 137.9, 134.0, 130.4, 130.2, 129.5, 128.6, 127.1, 126.1, 113.9, 55.4, 35.3, 35.1. GCMS (EI) calculated for $[\text{M}]^+$ 238.14 found 238.10. FTIR (neat, cm^{-1}): 3051(m), 3021(m), 2954(m), 2933(s), 2850(m), 1512(m), 1448(m), 1245(m), 1034(s), 837(s).



1-(2-Ethoxyethyl)-4-methoxybenzene (72) was isolated as a clear liquid (47.0 mg, 78%, >100:1 linear to branched ratio). ^1H NMR (300 MHz, CDCl_3) δ 7.15 (d, $J = 8.2$ Hz, 2H), 6.84 (d, $J = 8.3$ Hz, 2H), 3.79 (s, 3H), 3.70 – 3.38 (m, 4H), 2.84 (t, $J = 7.3$ Hz, 2H), 1.21 (t, $J = 7.0$ Hz, 3H). ^{13}C NMR (75 MHz, CDCl_3) δ 158.2, 131.3, 129.9, 114.0, 72.0, 66.3, 55.4, 35.7, 15.3. GCMS (EI) calculated for $[\text{M}]^+$ 180.12 found 180.10. FTIR (neat, cm^{-1}): 3028(m), 2991(m), 2974(m), 2934(m), 2864(m), 1613(m), 1513(s), 1247(s) 1111(m), 832(m).

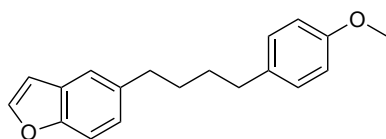


1-[2-(Benzyloxy)ethyl]-4-methoxybenzene (73) was isolated as a clear liquid (38.0 mg, 63%, 71:1 linear to branched ratio). ^1H NMR (300 MHz, CDCl_3) δ 7.41 – 7.27 (m, 5H), 7.16 (d, $J = 8.6$ Hz, 2H), 6.85 (d, $J = 8.6$ Hz, 2H), 4.54 (s, 2H), 3.80 (s, 3H), 3.67 (t, $J = 7.2$ Hz, 2H), 2.89 (t, $J = 7.2$ Hz, 2H). ^{13}C NMR (75 MHz, CDCl_3) δ 158.3, 138.6, 131.2, 130.0, 128.5, 127.7, 127.6, 114.0, 73.1, 71.7, 55.4, 35.6. GCMS (EI) calculated for $[\text{M}]^+$ 242.13 found 242.20. FTIR (neat, cm^{-1}): 3059(m), 3030(m) 2999(m), 2934(m), 2859 (m), 1612(m), 1513(s), 1247(s), 1100(m), 825(m).

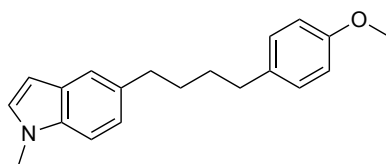


1-Methoxy-4-octylbenzene (74) was isolated as a clear liquid (35.0 mg, 56%, 10:1 linear to branched ratio). ^1H NMR (300 MHz, CDCl_3) δ 7.10 (d, $J = 8.5$ Hz, 2H), 6.83 (d, $J = 8.6$ Hz, 2H), 3.79 (s, 3H), 2.55 (t, $J = 7.5$ Hz, 2H), 1.67 – 1.46 (m, 2H), 1.40 – 1.16 (m, 10H), 0.89 (t, $J = 6.6$

Hz, 3H). ^{13}C NMR (126 MHz, CDCl_3) δ 157.7, 135.2, 129.4, 113.8, 55.4, 35.2, 32.1, 31.9, 29.6, 29.4, 22.8, 14.3. GCMS (EI) calculated for $[\text{M}]^+$ 220.18 found 220.20. FTIR (neat, cm^{-1}): 3051(m), 2997(m), 2927(s), 2855(m), 1613(m), 1512(s) 1247(s) 1041(m), 837(m).

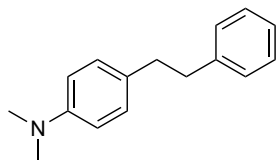


5-[4-(4-Methoxyphenyl)butyl]benzofuran (75) was isolated as a clear liquid (43.0 mg, 61%, 9:1 linear to branched ratio). ^1H NMR (500 MHz, CDCl_3) δ 7.60 (s, 1H), 7.46 – 7.36 (m, 2H), 7.10 (t, $J = 7.9$ Hz, 3H), 6.83 (d, $J = 7.9$ Hz, 2H), 6.71 (s, 1H), 3.80 (s, 3H), 2.73 (t, $J = 7.0$ Hz, 2H), 2.60 (t, $J = 6.8$ Hz, 2H), 1.83 – 1.59 (m, 4H). ^{13}C NMR (126 MHz, CDCl_3) δ 157.72, 153.57, 145.06, 137.12, 134.74, 129.32, 127.49, 124.99, 120.45, 113.74, 110.97, 106.43, 55.28, 35.76, 34.95, 31.69, 31.34. GCMS (EI) calculated for $[\text{M}]^+$ 280.37 found 280.10. FTIR (neat, cm^{-1}): 3113 (w), 3025 (m), 1998 (m), 2931 (m), 2855 (m), 1611 (m), 1511 (w), 1467 (m), 1246 (s), 1177 (m), 1126 (m), 1032 (m), 810 (m).

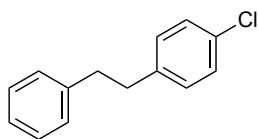


1-Methyl-5-[4-(4-methoxyphenyl)butyl]-1H-indole (76) was isolated as a pale orange solid (57.0 mg, 78%, 6:1 linear to branched ratio). ^1H NMR (300 MHz, CDCl_3) δ 7.45 (s, 1H), 7.29 (s, 1H), 7.18 – 6.98 (m, 4H), 6.87 (t, $J = 8.5$ Hz, 2H), 6.45 (d, $J = 2.9$ Hz, 1H), 3.82 (d, $J = 5.3$ Hz, 7H), 2.88 – 2.54 (m, 4H), 1.86 – 1.60 (m, 4H). ^{13}C NMR (75 MHz, CDCl_3) δ 157.87, 135.58, 135.11, 133.66, 129.47, 128.97, 128.88, 122.77, 120.18, 113.90, 109.04, 100.67, 55.46, 36.08,

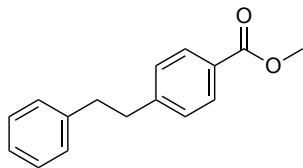
35.17, 32.98, 32.05, 31.56. GCMS (EI) calculated for $[M]^+$ 293.41 found 293.10. FTIR (neat, cm^{-1}): 3009 (w), 2929 (s), 2849 (m), 1611 (m), 1512 (s), 1245 (s), 1033 (m), 795 (m).



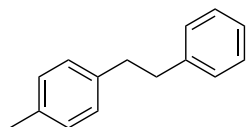
***N,N*-Dimethyl-4-phenethylamine (77)** was isolated as a white solid (48.0 mg, 85%, 19:1 linear to branched ratio). ^1H NMR (300 MHz, CDCl_3) δ 7.34 – 7.14 (m, 5H), 7.08 (d, $J = 8.5$ Hz, 2H), 6.70 (d, $J = 8.5$ Hz, 2H), 3.04 – 2.75 (m, 10H). ^{13}C NMR (75 MHz, CDCl_3) δ 149.3, 142.4, 130.2, 129.1, 128.6, 128.4, 125.9, 113.1, 41.0, 38.4, 37.1. GCMS (EI) calculated for $[M]^+$ 225.15 found 225.20. FTIR (neat, cm^{-1}): 3059(m), 3026(m), 2919(m), 2853(m), 1616(m), 1522(s), 1346(m), 810(m).



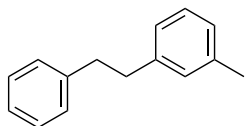
1-Chloro-4-phenethylbenzene (78) was isolated as a white solid (24.9 mg, 46%, 15:1 linear to branched ratio). ^1H NMR (500 MHz, CDCl_3) δ 7.35 (t, $J = 7.3$ Hz, 2H), 7.33 – 7.25 (m, 3H), 7.23 (d, $J = 7.5$ Hz, 2H), 7.15 (d, $J = 8.1$ Hz, 2H), 2.97 (s, 4H). ^{13}C NMR (126 MHz, CDCl_3) δ 141.4, 140.2, 131.8, 130.0, 128.6, 128.5, 128.5, 126.2, 37.9, 37.3. GCMS (EI) calculated for $[M]^+$ 216.07 found 216.10. FTIR (neat, cm^{-1}): 3028(m), 2926(m), 2859(m), 1604(m), 1492(s), 1093(m), 813(m), 699(s).



Methyl-4-phenethylbenzoate (79) was isolated as a clear liquid (25.7 mg, 43%, 24:1 linear to branched ratio). ^1H NMR (500 MHz, CDCl_3) δ 8.03 (d, $J = 7.5$ Hz, 1H), 7.40 – 7.25 (m, 3H), 7.23 (d, $J = 7.4$ Hz, 1H), 3.97 (s, 2H), 3.11 – 2.90 (m, 2H). ^{13}C NMR (126 MHz, CDCl_3) δ 167.2, 147.3, 141.2, 129.8, 128.6, 128.5, 128.5, 128.0, 126.2, 52.1, 38.0, 37.5. GCMS (EI) calculated for $[\text{M}]^+$ 240.12 found 240.10. FTIR (neat, cm^{-1}): 3062(w), 3028(m), 2950(m), 2925(m), 2859(w), 1723(s), 1612(m), 1435(m), 1280(s), 1111(m), 700(s).

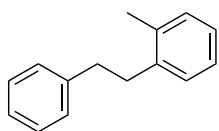


1-Methyl-4-phenethylbenzene (80) was isolated as a white solid (42.0 mg, 86%, 55:1 linear to branched ratio). ^1H NMR (300 MHz, CDCl_3) δ 7.42 – 7.19 (m, 5H), 7.13 (s, 4H), 2.94 (s, 4H), 2.37 (s, 3H). ^{13}C NMR (126 MHz, CDCl_3) δ 142.1, 138.9, 135.5, 129.2, 128.6, 128.5, 126.0, 38.2, 37.7, 21.2. GCMS (EI) calculated for $[\text{M}]^+$ 196.13 found 196.10. FTIR (neat, cm^{-1}): 3051(m), 3026(s), 2924(s), 2857(m), 1516(s), 1454(s), 837(s).

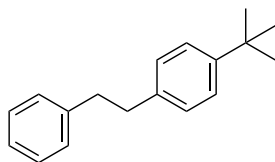


1-Methyl-3-(2-phenethyl)benzene (81) was isolated as a clear liquid (32.6 mg, 66%, 71:1 linear to branched ratio). ^1H NMR (500 MHz, CDCl_3) δ 7.42 – 7.35 (m, 2H), 7.33 – 7.26 (m, 4H), 7.15 – 7.07 (m, 3H), 3.11 – 2.89 (m, 4H), 2.43 (s, 3H). ^{13}C NMR (126 MHz, CDCl_3) δ 142.0, 141.8,

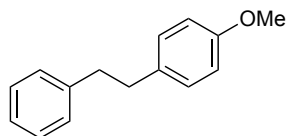
137.9, 129.4, 128.5, 128.4, 128.4, 126.8, 126.0, 125.6, 38.1, 38.0, 21.5. GCMS (EI) calculated for $[M]^+$ 196.13 found 196.10. FTIR (neat, cm^{-1}): 3085(m), 3061(m), 3026(s), 2922(s), 2859(m), 1605(m), 1496(s), 1454(s), 780(s).



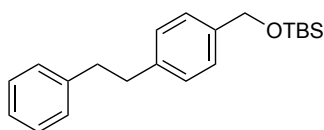
1-Methyl-3-phenethylbenzene (82) was isolated as a clear liquid (38.3 mg, 78%, 44:1 linear to branched ratio). ^1H NMR (500 MHz, CDCl_3) δ 7.48 – 7.45 (m, 2H), 7.39 – 7.37 (m, 3H), 7.32 – 7.30 (m, 4H), 3.22 – 2.98 (m, 4H), 2.48 (s, 3H). ^{13}C NMR (126 MHz, CDCl_3) δ 142.1, 140.1, 136.0, 130.3, 128.9, 128.5, 128.5, 126.2, 126.1, 126.2, 36.9, 35.5, 19.4. GCMS (EI) calculated for $[M]^+$ 196.13 found 196.10. FTIR (neat, cm^{-1}): 3062(m), 3026(s), 2943(s), 2865(m), 1603(m), 1495(s), 1454(s), 754(s).



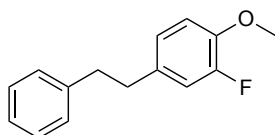
1-(*Tert*-butyl)-4-phenethylbenzene (83) was isolated as a white solid (48.5 mg, 81%, 65:1 linear to branched ratio). ^1H NMR (300 MHz, CDCl_3) δ 7.49 – 7.12 (m, 9H), 2.99 (s, 4H), 1.39 (s, 9H). ^{13}C NMR (75 MHz, CDCl_3) δ 148.9, 142.2, 138.9, 128.6, 128.5, 128.2, 126.0, 125.4, 38.0, 37.5, 34.5, 31.6. GCMS (EI) calculated for $[M]^+$ 238.17 found 238.20. FTIR (neat, cm^{-1}): 3087(w), 3062(m), 3027(m), 2963(w), 2863(m), 1605(m), 1516(m), 1455(m), 820(s).



1-Methoxy-4-(2-phenylethyl)benzene (84) from bromoanisole was isolated as a white solid (53.0 mg, 99%, 22:1 linear to branched ratio). Spectral data matched that reported above (**50**).

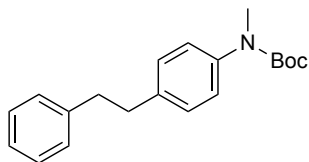


1-[(*Tert*-butyl)dimethylsilyloxy]-4-phenethylbenzene (85) was isolated as a clear liquid (57.0 mg, 70%, 31:1 linear to branched ratio). ^1H NMR (300 MHz, CDCl_3) δ 7.46 – 7.08 (m, 9H), 4.79 (s, 2H), 2.98 (s, 4H), 1.01 (s, 9H), 0.17 (s, 6H). ^{13}C NMR (75 MHz, CDCl_3) δ 142.01, 140.60, 139.24, 128.65, 128.48, 126.40, 126.07, 65.11, 38.14, 37.76, 26.17, 18.61, -5.02. GCMS (EI) calculated for $[\text{M}]^+$ 326.56 found 326.20. FTIR (neat, cm^{-1}): 3062 (w), 3026 (m), 2954 (s), 2884 (m), 2856 (s), 1605 (m), 1471 (m), 1257 (m), 1090 (s), 838 (s), 777 (m).

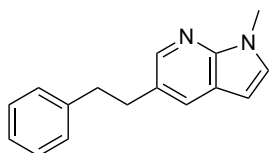


1-Fluoro-2-methoxy-5-phenethylbenzene (86) was isolated as a crystalline white solid (42.0 mg, 73%, 44:1 linear to branched ratio). ^1H NMR (500 MHz, CDCl_3) δ 7.29 (t, $J = 7.5$ Hz, 2H), 7.23 – 7.14 (m, 3H), 6.95 – 6.80 (m, 3H), 3.87 (s, 3H), 3.09 – 2.70 (m, 4H). ^{13}C NMR (75 MHz, CDCl_3) δ 154.16, 145.97 (d, $J = 10.8$ Hz), 141.56, 140.21 (d, $J = 1614.4$ Hz), 135.18, 128.58 (d, $J = 6.7$ Hz), 126.18, 124.09, 116.33 (d, $J = 17.7$ Hz), 113.78, 56.62, 37.96, 37.04. GCMS (EI) calculated

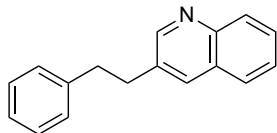
for $[M]^+$ 230.28 found 230.10. FTIR (neat, cm^{-1}): 3061 (w), 3026 (m), 2933 (m), 2838 (m), 1518 (s), 1276 (s), 1224 (m), 1123 (m), 1030 (m), 805 (m).



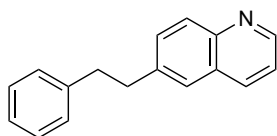
1-*N*-methyl-*N*-(tert-butyloxycarbonyl)-4-phenethylbenzene (87) was isolated as a clear liquid (63.0 mg, 81%, 41:1 linear to branched ratio). ^1H NMR (300 MHz, CDCl_3) δ 7.43 – 6.79 (m, 9H), 3.23 (s, $J = 6.1$ Hz, 3H), 2.89 (s, 4H), 1.44 (s, $J = 9.1$ Hz, 9H). ^{13}C NMR (75 MHz, CDCl_3) δ 155.12, 142.03, 141.86, 139.12, 128.76, 128.65, 128.51, 126.12, 125.64, 80.28, 38.02, 37.54, 28.56. GCMS (EI) calculated for $[M]^+$ 311.43 found 311.00. FTIR (neat, cm^{-1}): 3060 (w), 3027 (m), 2974 (m), 2931 (m), 1699 (s), 1599 (w), 1514 (m), 1365 (m), 1121 (m), 1038 (m), 746 (m).



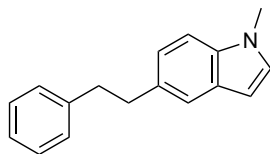
1-Methyl-5-[2-phenylethyl]-1*H*-pyrrolo[2,3-*b*]pyridine-5-yl (88) was isolated as a clear liquid (46.0 mg, 78%, 13:1 linear to branched ratio). ^1H NMR (300 MHz, CDCl_3) δ 8.16 (d, $J = 1.9$ Hz, 1H), 7.68 (d, $J = 2.0$ Hz, 1H), 7.39 – 7.10 (m, 6H), 6.37 (d, $J = 3.4$ Hz, 1H), 3.86 (s, 3H), 3.11 – 2.84 (m, 4H). ^{13}C NMR (75 MHz, CDCl_3) δ 147.09, 143.73, 141.68, 129.31, 128.67, 128.52, 128.41, 126.13, 120.53, 98.99, 38.75, 35.30, 31.39. GCMS (EI) calculated for $[M]^+$ 236.32 found 236.10. FTIR (neat, cm^{-1}): 3059 (w), 3024 (m), 2921 (m), 2856 (m), 1603 (m), 1515 (s), 1402 (s), 1353 (m), 1298 (m), 1081 (m), 700 (s).



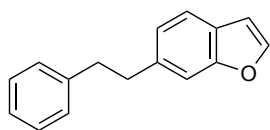
3-(2-phenylethyl)quinoline (89) was isolated as a white solid (26.0 mg, 44%, 21:1 linear to branched ratio). ^1H NMR (500 MHz, CDCl_3) δ 8.79 (s, 1H), 8.13 (d, $J = 8.3$ Hz, 1H), 7.89 (s, 1H), 7.77 (d, $J = 8.1$ Hz, 1H), 7.69 (t, $J = 7.6$ Hz, 1H), 7.55 (t, $J = 7.4$ Hz, 1H), 7.38 – 7.15 (m, 5H), 3.23 – 2.97 (m, 4H). ^{13}C NMR (126 MHz, CDCl_3) δ 152.11, 147.02, 140.91, 134.54, 134.31, 129.31, 128.80, 128.63, 128.22, 127.80, 127.49, 126.70, 126.38, 37.56, 35.22. GCMS (EI) calculated for $[\text{M}]^+$ 233.31 found 233.10. FTIR (neat, cm^{-1}): 3061 (m), 3026 (m), 2926 (m), 2856 (m), 1603 (m), 1570 (m), 1404 (m), 1453 (m), 1329 (m), 1125 (m), 750 (s).



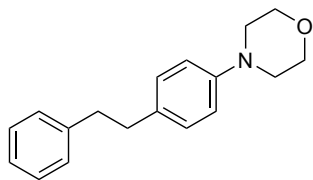
6-(2-phenylethyl)quinoline (90) was isolated as a white solid (41.0 mg, 70%, 11:1 linear to branched ratio). ^1H NMR (500 MHz, CDCl_3) δ 8.91 (s, 1H), 8.09 (t, $J = 8.3$ Hz, 2H), 7.60 (dd, $J = 10.6, 1.7$ Hz, 2H), 7.39 (dd, $J = 8.2, 4.2$ Hz, 1H), 7.35 – 7.27 (m, 2H), 7.24 (dd, $J = 11.4, 7.2$ Hz, 3H), 3.15 (dd, $J = 9.4, 6.3$ Hz, 2H), 3.06 (dd, $J = 9.4, 6.2$ Hz, 2H). ^{13}C NMR (126 MHz, CDCl_3) δ 149.87, 147.35, 141.46, 140.26, 135.72, 131.12, 129.48, 128.62, 128.55, 127.86, 126.43, 126.21, 121.25, 37.96, 37.77. GCMS (EI) calculated for $[\text{M}]^+$ 233.31 found 233.10. FTIR (neat, cm^{-1}): 3059 (w), 3024 (m), 2922 (m), 2855 (m), 1602 (m), 1493 (s), 1452 (m), 1305 (w), 1219 (m), 830 (m).



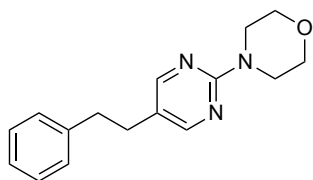
1-Methyl-5-(2-phenylethyl)-1H-indole (91) was isolated as a red solid (56.0 mg, 94%, 36:1 linear to branched ratio). ^1H NMR (300 MHz, CDCl_3) δ 7.50 (s, 1H), 7.42 – 7.20 (m, 6H), 7.13 (dd, $J = 8.3, 1.4$ Hz, 1H), 7.07 (d, $J = 3.0$ Hz, 1H), 6.47 (d, $J = 2.8$ Hz, 1H), 3.81 (s, 3H), 3.17 – 2.87 (m, 4H). ^{13}C NMR (126 MHz, CDCl_3) δ 142.51, 135.60, 132.89, 129.09, 128.83, 128.67, 128.46, 125.93, 122.68, 120.20, 109.15, 100.66, 39.10, 38.31, 33.01. GCMS (EI) calculated for $[\text{M}]^+$ 235.33 found 235.10. FTIR (neat, cm^{-1}): 3100 (m), 3083 (m), 3060 (s), 3024 (s), 2922 (s), 2855 (s), 2818 (m), 1602 (m), 1513 (s), 1494 (s), 1453 (m), 1422 (s), 1338 (s), 1244 (s), 1078 (s), 877 (m).



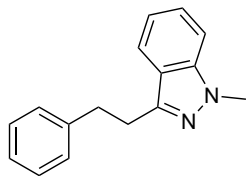
6-(2-phenylethyl)benzofuran (92) was isolated as a clear liquid (42.0 mg, 76%, 41:1 linear to branched ratio). ^1H NMR (300 MHz, CDCl_3) δ 7.58 (d, $J = 2.2$ Hz, 1H), 7.51 (d, $J = 7.9$ Hz, 1H), 7.42 – 7.16 (m, 6H), 7.10 (dd, $J = 8.0, 1.1$ Hz, 1H), 6.74 (d, $J = 1.3$ Hz, 1H), 3.26 – 2.91 (m, 4H). ^{13}C NMR (126 MHz, CDCl_3) δ 155.48, 144.75, 141.85, 138.66, 128.65, 128.53, 126.12, 125.52, 123.78, 120.92, 111.21, 106.55, 38.48, 38.24. GCMS (EI) calculated for $[\text{M}]^+$ 222.29 found 222.10. FTIR (neat, cm^{-1}): 3061 (m), 3026 (m), 2924 (m), 2857 (m), 1619 (m), 1496 (m), 1430 (m), 1267 (m), 1142 (m), 1028 (m), 811 (m).



1-Morpholinyl-4-(2-phenylethyl)benzene (93) was isolated as a white solid (62.0 mg, 93%, 26:1 linear to branched ratio). ^1H NMR (300 MHz, CDCl_3) δ 7.39 – 7.16 (m, 5H), 7.11 (d, $J = 8.5$ Hz, 2H), 6.86 (d, $J = 8.6$ Hz, 2H), 4.09 – 3.70 (m, 4H), 3.33 – 3.06 (m, 4H), 2.99 – 2.77 (m, 4H). ^{13}C NMR (75 MHz, CDCl_3) δ 149.77, 142.14, 133.66, 129.31, 128.64, 128.47, 126.01, 116.07, 67.15, 49.94, 38.22, 37.13. GCMS (EI) calculated for $[\text{M}]^+$ 267.37 found 267.10. FTIR (neat, cm^{-1}): 3027 (w), 2960 (s), 2915 (s), 2838 (s), 1677 (s), 16117 (m), 1515 (s), 1455 (s), 1265 (s), 1124 (s), 1124 (s), 930 (s), 810 (s).



4-[2-[2-(4-morpholinyl)-5-pyrimidinyl]ethyl]benzene (94) was isolated as a (47.0 mg, 70%, 8:1 linear to branched ratio). ^1H NMR (300 MHz, CDCl_3) δ 8.10 (s, 2H), 7.33 – 7.24 (m, 2H), 7.24 – 7.18 (m, 1H), 7.18 – 7.11 (m, 2H), 3.75 (s, 8H), 2.96 – 2.65 (m, 4H). ^{13}C NMR (126 MHz, CDCl_3) δ 161.12, 157.75, 140.85, 128.68, 128.67, 126.40, 122.82, 67.00, 44.60, 37.71, 31.54. GCMS (EI) calculated for $[\text{M}]^+$ 269.35 found 269.10. FTIR (neat, cm^{-1}): 2968 (m), 2915 (m), 2895 (m), 2857 (m), 1605 (s), 1493 (s), 1445 (m), 1357 (m), 1305 (m), 1255 (m), 1117 (s), 1959 (m), 795 (m).



1-Methyl-3-(2-phenylethyl)-1H-indazole (95) was isolated as a (47.0 mg, 69%, 21:1 linear to branched ratio). ^1H NMR (500 MHz, CDCl_3) δ 8.21 (d, $J = 1.1$ Hz, 1H), 7.73 (d, $J = 1.7$ Hz, 1H), 7.31 (dd, $J = 14.1, 7.0$ Hz, 2H), 7.24 (t, $J = 7.0$ Hz, 3H), 7.18 (d, $J = 3.4$ Hz, 1H), 6.41 (d, $J = 3.4$ Hz, 1H), 3.91 (s, 3H), 3.17–2.91 (m, 4H). ^{13}C NMR (126 MHz, CDCl_3) δ 147.00, 143.69, 141.67, 129.36, 128.68, 128.53, 128.48, 126.15, 120.53, 98.97, 38.79, 35.32, 31.45. GCMS (EI) calculated for $[\text{M}]^+$ 236.32 found 236.10. FTIR (neat, cm^{-1}): 3024 (m), 2922 (m), 2856 (m), 1603 (m), 1514 (s), 1493 (m), 1402 (s), 1351 (m), 1081 (m), 700 (s).

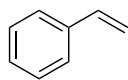
2.6.5 *Synthesis and Characterization of Alkene Starting Material*

General Procedure A for the synthesis of alkenes

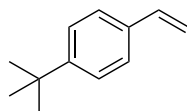
A flamed dried 25 mL round bottom flask was allowed to cool under nitrogen, and then was charged with a stir bar, methyltriphenylphosphonium bromide (1.1 g, 3.0 mmol, 1.0 equiv) and THF (0.5 M). The suspension was cooled down to 0°C and n-butyl-lithium (1.4 ml, 3.6 mmol, 1.2 equiv, 2.5 M in hexanes) or potassium tert-butoxide (4.5 ml, 4.5 mmol, 1.5 equiv, 1.0 M in THF) was added slowly. The reaction was allowed to warm up to room temperature and was stirred for 10 minutes. The reaction was then cooled down to 0°C again and aldehyde (3.0 mmol, 1.1 equiv) was added slowly. The reaction was stirred at room temperature overnight. The reaction mixture was then filtered and the filtrate was concentrated under vacuum. The product was purified via flash chromatography.

General Procedure B for the synthesis of alkenes

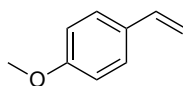
A dry and argon flushed 50 mL Schlenk-tube is charged with the aryl bromide (2.5 mmol, 1.0 equiv), Pd₂dba₃ (0.25 mmol, 0.05 equiv), RuPhos (0.50 mmol, 0.10 equiv) and toluene (0.5 M). After stirring the reaction mixture for 5 min, alkenyl zinc chloride (5.0 mmol, 2.0 equiv, 1 M in THF) is added (mildly exothermic). The reaction mixture was heated to 75 °C for overnight, during which time the color had progressed to dark brown/black. Then, the reaction mixture was cooled to room temperature and quenched with a saturated aqueous NH₄Cl solution and extracted with 1:1 v/v hexanes/ethyl acetate. The organic layer was washed with brine, dried over sodium sulfate, and the solvent was removed by rotary evaporation under reduced pressure. The crude residue was purified by silica gel chromatography.



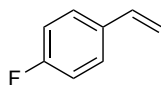
Styrene (48) was purchased from TCI Chemicals USA and was used as received.



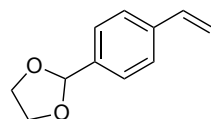
4-tert-Butylstyrene (103) was purchased from Sigma-Aldrich and was used as received.



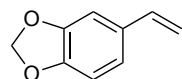
4-Vinylanisole (104) was synthesized using General Procedure A and has been previously characterized.⁴³



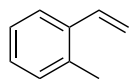
4-Fluorostyrene (105) was synthesized using General Procedure A and has been previously characterized.⁴⁴



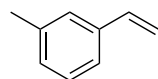
2-(4-Ethenylphenyl)-1,3-dioxolane (106) was synthesized using General Procedure A and has been previously characterized.⁴⁵



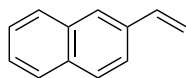
5-Ethenyl-1,3-benzodioxole (107) was synthesized using General Procedure A and has been previously characterized.⁴⁶



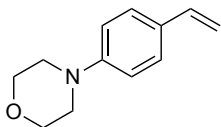
1-Ethenyl-2-methylbenzene (108) was synthesized using General Procedure A and has been previously characterized.⁴⁴



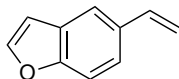
1-Ethenyl-3-methylbenzene (109) was synthesized using General Procedure A and has been previously characterized.⁴³



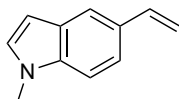
2-Ethenylnaphthalene (110) was synthesized using General Procedure A and has been previously characterized.⁴⁷



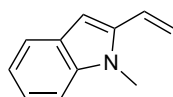
4-(4-Ethenylphenyl)-morpholine (111) was synthesized using General procedure A and has been previously characterized.⁴⁸



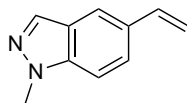
5-Ethenylbenzofuran (112) was synthesized using General procedure A and has been previously characterized.⁴⁹



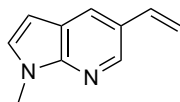
5-Ethenyl-1-methyl-1H-indole (113) was synthesized using General procedure A and has been previously characterized.⁵⁰



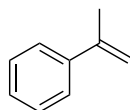
2-Ethenyl-1-methyl-1H-indole (114) was synthesized using General procedure A and has been previously characterized.⁵¹



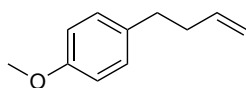
5-Ethenyl-1-methyl-1*H*-indazole (115) was synthesized using General procedure A and has been previously characterized.⁵²



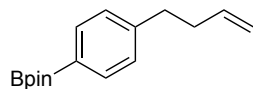
5-Ethenyl-1-methyl-1*H*-pyrrolo[2,3-*b*]pyridine (116) was synthesized using General procedure A and isolated as a clear liquid (88 mg, 62% yield). ¹H NMR (500 MHz, CDCl₃) δ 8.38 (s, 1H), 7.96 (s, 1H), 7.16 (d, *J* = 3.2 Hz, 1H), 6.83 (dd, *J* = 17.6, 11.0 Hz, 1H), 6.43 (d, *J* = 3.3 Hz, 1H), 5.76 (d, *J* = 17.6 Hz, 1H), 5.23 (d, *J* = 11.0 Hz, 1H), 3.88 (s, 3H).



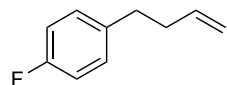
Isopropenylbenzene (117) was purchased from TCI Chemicals USA and was used as received.



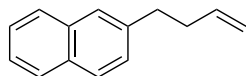
1-(3-Buten-1-yl)-4-methoxybenzene (118) was synthesized using General Procedure B and has been previously characterized.⁵³



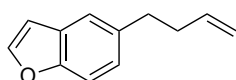
2-[4-(3-Buten-1-yl)phenyl]-4,4,5,5-tetramethyl-1,3,2-dioxaborolane (119) was synthesized using General Procedure B and has been previously characterized.⁵⁴



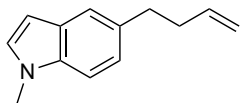
1-(3-Buten-1-yl)-4-fluorobenzene (120) was synthesized using General Procedure B and has been previously characterized.⁴⁸



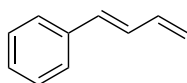
2-(3-Buten-1-yl)naphthalene (121) was synthesized using General Procedure B and has been previously characterized.⁵⁵



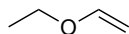
5-(3-Buten-1-yl)benzofuran (122) was synthesized using General Procedure B and isolated as a clear oil (233 mg, 74% yield). ¹H NMR (300 MHz, CDCl₃) δ 7.62 (d, J = 2.1 Hz, 1H), 7.44 (d, J = 8.2 Hz, 2H), 7.34 – 7.10 (m, 2H), 6.74 (d, J = 1.9 Hz, 1H), 5.91 (ddt, J = 16.9, 10.2, 6.6 Hz, 1H), 5.17 – 4.90 (m, 2H), 2.90 – 2.74 (m, 2H), 2.44 (dd, J = 15.0, 7.2 Hz, 2H).



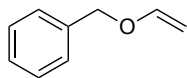
5-(3-Buten-1-yl)-1-methyl-1*H*-indole (123) was synthesized using General Procedure B and isolated as a yellow oil (178 mg, 59% yield). ^1H NMR (300 MHz, CDCl_3) δ 7.46 (s, 1H), 7.28 (s, 1H), 7.10 (dd, $J = 8.4, 1.2$ Hz, 1H), 7.05 (d, $J = 3.1$ Hz, 1H), 6.45 (d, $J = 2.9$ Hz, 1H), 5.94 (ddt, $J = 16.9, 10.2, 6.6$ Hz, 1H), 5.19 – 4.91 (m, 2H), 3.80 (s, 3H), 2.90 – 2.75 (m, 2H), 2.45 (dt, $J = 14.4, 7.0$ Hz, 2H).



1,3-Butadien-1-yl-benzene (124) was synthesized using General Procedure A and has been previously characterized.⁵⁶



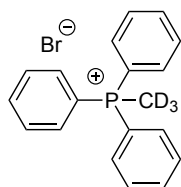
Ethoxyethene (125) was purchased from TCI Chemicals USA and was used as received.



[(Ethenyloxy)methyl]benzene (126)

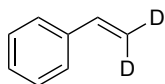
To a screw cap tube containing AuClPPh_3 (29.7 mg, 2 mol%, 0.06 mmol) and silver acetate (10 mg, 2.0 mol%, 0.06 mmol), ethyl vinyl ether (2.9 mL, 10 equiv, 30 mmol) was added. The mixture was stirred at room temperature for 10 min. Benzyl alcohol (3 mmol) was added and the mixture was stirred at 50 °C overnight. The crude material was concentrated under reduced pressure and

purified on a silica gel column to give a clear oil (267 mg, 66%). This product has been previously characterized.⁵⁷



Methyl-d₃-triphenylphosphonium bromide (127)

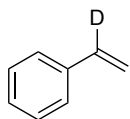
A dram vial was charged with a stir bar, triphenylphosphonium bromide (1.8 g, 1.0 equiv, 5 mmol), D₂O (10 mL), and NaOH (0.10 g, 0.5 equiv, 2.5 mmol). The mixture was allowed to stir for 24 h at room temperature, after which dichloromethane was added. The organic fraction was collected and dried with MgSO₄. The resulting solution was layered with hexanes and the mixture was filtered to give a white crystalline solid (1.3 g, 74%, 80% deuterium incorporation). The spectral data matched those that were previously reported.⁵⁸



Styrene-β,β-d₂ (48-βD)

A flamed dried 25 mL round bottom flask cooled under nitrogen, and then was charged with a stir bar, methyl-d₃-triphenylphosphonium bromide (**S16**) (0.72 g, 2.0 mmol, 1.0 equiv) and THF (0.5 M). The suspension was cooled down to 0°C and n-butyl-lithium (0.96, 2.4 mmol, 1.2 equiv, 2.5 M in hexanes) was added slowly. The reaction was warmed up to room temperature and was stirred for 10 minutes. The reaction was then cooled down to 0°C again and benzaldehyde (0.20 ml, 2.0 mmol, 1.0 equiv) was added slowly. The reaction was stirred at room temperature overnight. The reaction mixture was then filtered and the filtrate was concentrated under vacuum.

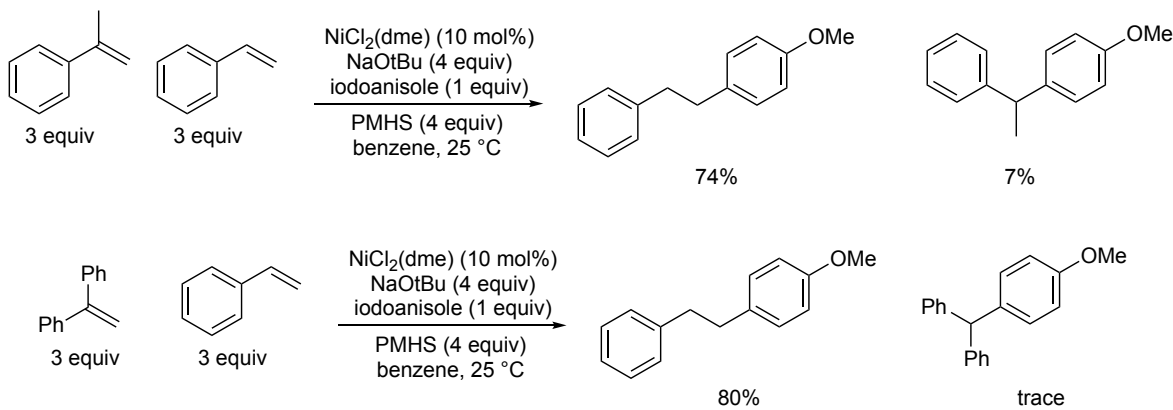
The product was purified via flash chromatography to give a clear liquid (73 mg, 34%, 80% deuterium incorporation). The spectral data matched those that were previously reported.⁵⁹



Styrene- α -d₁ (48- α D) was purchased from Sigma-Aldrich and was used as received.

2.6.6 Mechanistic Experiments

Competition Experiments (Scheme 2.3)



Procedure for competition experiments:

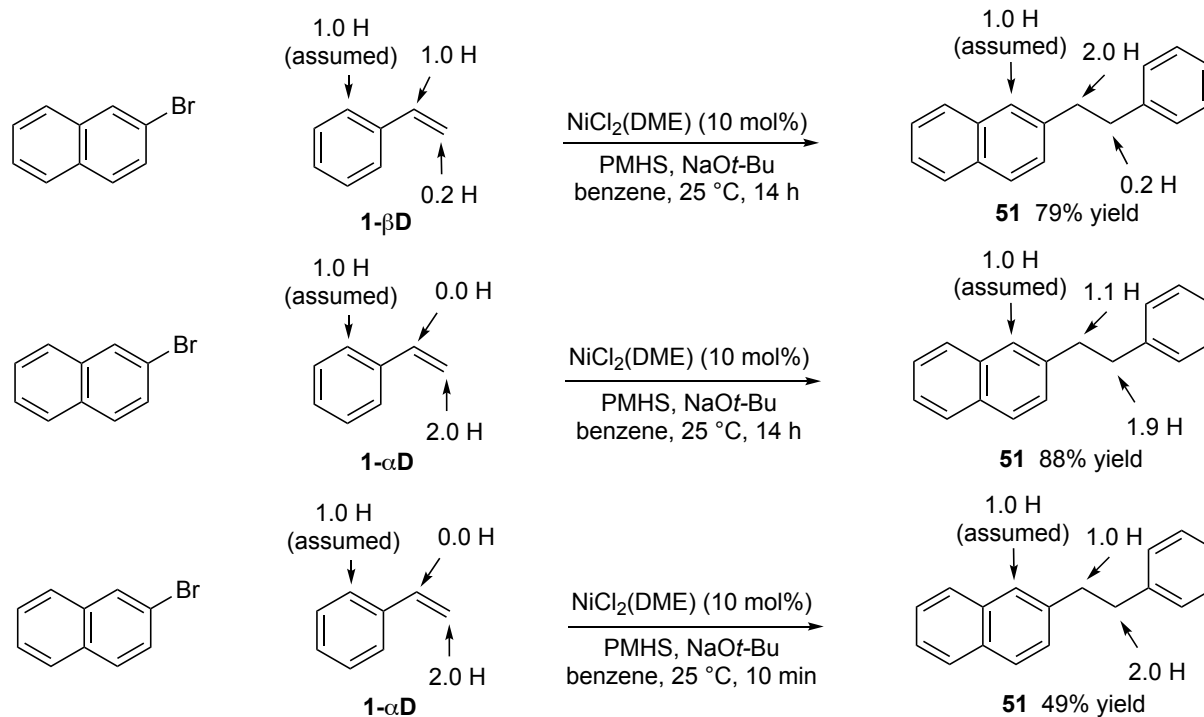
In a nitrogen filled glovebox, a dram vial was charged with a stir bar, and NiCl₂(dme) (5.5 mg, 0.025 mmol, 10 mol%). Stock solutions of PMHS, alkenes, and the aryl halide were prepared in benzene at 0.5 mg/ μ L concentrations. A stock solution of NaO*t*-Bu was prepared in benzene at a concentration of 0.1 mg/ μ L. PMHS (12 mg, 0.20 mmol, 4.0 equiv), styrene (15.6 mg, 0.15 mmol, 3.0 equiv), the other alkene (0.15 mmol, 3.0 equiv) and iodoanisole (11.7 mg, 0.05 mmol, 1.0 equiv). NaO*t*-Bu (19.1 mg, 0.20 mmol, 4.0 equiv) was added last. The reaction mixture was left

to stir at room temperature for 14 h. Mesitylene (6.0 mg, 0.05 mmol, 1.0 equiv) was then added. A 30 μ L aliquot was taken from the reaction mixture and filtered through a small plug of silica and rinsed with dichloromethane. Yields were determined by GC analysis.

Experimental Procedure for Reaction Shown in Scheme 2b

In a nitrogen filled glovebox, a dram vial was charged with a stir bar, and $\text{NiCl}_2(\text{dme})$ (5.5 mg, 0.025 mmol, 10 mol%). Stock solutions of PMHS, alkenes, and the aryl halide were prepared in benzene at 0.5 mg/ μ L concentrations. A stock solution of NaOt-Bu was prepared in benzene at a concentration of 0.1 mg/ μ L. PMHS (60.1 mg, 1.0 mmol, 4.0 equiv), 2-ethenylnaphthalene (77.1 mg, 0.50 mmol, 2.0 equiv), and iodoanisole (58.5 mg, 0.25 mmol, 1.0 equiv) were added in rapid succession. Ethanol (29.2 μ L, 0.50 mmol, 2.0 equiv) was added and then NaOt-Bu (96.1 mg, 1.0 mmol, 4.0 equiv) was immediately added. The reaction mixture was left to stir at room temperature for 14 h. Mesitylene (30.0 mg, 0.25 mmol, 1.0 equiv) was then added. A 30 μ L aliquot was taken from the reaction mixture and filtered through a small plug of silica and rinsed with dichloromethane. Yields were determined by GC analysis.

Experimental Procedure for Deuterium Scrambling Experiments (Scheme 2.5)



In a nitrogen filled glovebox, a dram vial was charged with a stir bar, and $\text{NiCl}_2(\text{dme})$ (5.5 mg, 0.025 mmol, 10 mol%). Stock solutions of PMHS, alkenes, and the aryl halide were prepared in benzene at 0.5 mg/ μL concentrations. A stock solution of NaOt-Bu was prepared in benzene at a concentration of 0.1 mg/ μL . PMHS (60.1 mg, 1.0 mmol, 4.0 equiv), deuterated styrene (0.50 mmol, 2.0 equiv), and bromonaphthalene (51.8 mg, 0.25 mmol, 1.0 equiv) were added in rapid succession. NaOt-Bu (96.1 mg, 1.0 mmol, 4.0 equiv) was immediately added. The reaction mixture was left to stir at room temperature for 14 h or 10 minutes. Mesitylene (30.0 mg, 0.25 mmol, 1.0 equiv) was then added. A 30 μL aliquot was taken from the reaction mixture and filtered through a small plug of silica and rinsed with dichloromethane. Yields were determined by GC analysis. Deuterium incorporation was determined by ^1H NMR analysis.

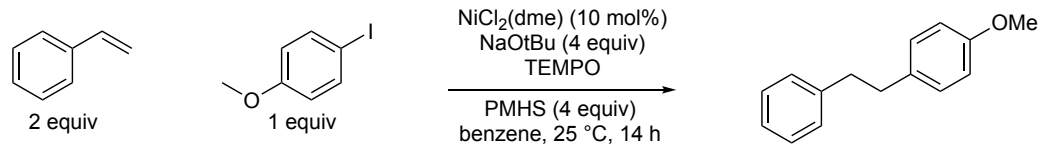
Experimental Procedure for the Reaction Shown in Scheme 2e

In a nitrogen filled glovebox, a dram vial was charged with a stir bar, and NiCl₂(dme) (1.1 mg, 0.005 mmol, 10 mol%). Stock solutions of PMHS, alkenes, and the aryl halide were prepared in benzene at 0.5 mg/μL concentrations. A stock solution of NaO*t*-Bu was prepared in benzene at a concentration of 0.1 mg/μL. PMHS (6.0 mg, 0.20 mmol, 4.0 equiv), styrene (10.4 mg, 0.10 mmol, 2.0 equiv), and iodoanisole (11.7 mg, 0.05 mmol, 1.0 equiv) were added in rapid succession. Mercury (44.5 μL, 3.0 mmol, 60 equiv) was added and then NaO*t*-Bu (19.2 mg, 0.20 mmol, 4.0 equiv) was immediately added. The reaction mixture was left to stir at room temperature for 14 h. Mesitylene (6.0 mg, 0.05 mmol, 1.0 equiv) was then added. A 30 μL aliquot was taken from the reaction mixture and filtered through a small plug of silica and rinsed with dichloromethane. Yields were determined by GC analysis.

Experimental Procedure for TEMPO Experiments

In a nitrogen filled glovebox, a dram vial was charged with a stir bar, and NiCl₂(dme) (1.1 mg, 0.005 mmol, 10 mol%). Stock solutions of PMHS, alkenes, and the aryl halide were prepared in benzene at 0.5 mg/μL concentrations. A stock solution of NaO*t*-Bu was prepared in benzene at a concentration of 0.1 mg/μL. PMHS (6.0 mg, 0.20 mmol, 4.0 equiv), styrene (10.4 mg, 0.10 mmol, 2.0 equiv), and iodoanisole (11.7 mg, 0.05 mmol, 1.0 equiv) were added in rapid succession. TEMPO was added and then NaO*t*-Bu (19.2 mg, 0.20 mmol, 4.0 equiv) was immediately added. The reaction mixture was left to stir at room temperature for 14 h. Mesitylene (6.0 mg, 0.05 mmol, 1.0 equiv) was then added. A 30 μL aliquot was taken from the reaction mixture and filtered through a small plug of silica and rinsed with dichloromethane. Yields were determined by GC analysis.

Table 2.9. TEMPO Experiments



Entry	TEMPO Equiv	Yield (%)
1	0.1	63
2	0.5	0
3	1.0	0

BIBLIOGRAPHY

- (1) D. J. Gorin, F. D. Toste, *Nature* **2007**, *446* (7134), 395-403; D. Pflästerer, A. S. Hashmi, *Chem. Soc. Rev.* **2015**; A. S. Hashmi, M. Rudolph, *Chem. Soc. Rev.* **2008**, *37* (9), 1766-1775; C. Obradors, A. Echavarren, *Chem. Comm.* **2014**, *50* (1), 16-28.
- (2) J. Teles, S. Brode, M. Chabanas, *Angew. Chem. Int. Ed.* **1998**, *37* (10), 1415-1418.
- (3) F. D. Toste, V. R. Michelet, *Gold catalysis : an homogeneous approach*. Imperial College Press World Scientific Publishing Co. Pte: London, 2014; p xvii, 545 pages.
- (4) P. Pyykko, *Chem. Soc. Rev.* **2008**, *37* (9), 1967-1997.
- (5) A. Furstner, P. Davies, *Angew. Chem. Int. Ed.* **2007**, *46*, 3410-3449; M. Rudolph, A. Hashmi, *Chem. Soc. Rev.* **2012**, *41*, 2448-2462; L. Liu, G. Hammond, *Chem. Soc. Rev.* **2012**, *41*, 3129-3139;
- (6) W. Yang, A. Hashmi, *Chem. Soc. Rev.* **2014**, *43*, 2941-2955; J. Akana, K. Bhattacharyya, P. Muller, J. Sadighi, *J. Am. Chem. Soc.* **2007**, *129*, 7736-+; O. Egorova, H. Seo, Y. Kim, D. Moon, Y. Rhee, K. Ahn, *Angew. Chem. Int. Ed.* **2011**, *50*, 11446-11450; A. Hashmi, A. Schuster, S. Gaillard, L. Cavallo, A. Poater, S. Nolan, *Organometallics* **2011**, *30*, 6328-6337.
- (7) C. Nieto-Oberhuber, M. Munoz, E. Bunuel, C. Nevado, D. Cardenas, A. Echavarren, *Angew. Chem. Int. Ed.* **2004**, *43*, 2402-2406; L. Zhang, *J. Am. Chem. Soc.* **2005**, *127*, 16804-16805; C. Li, K. Pati, G. Lin, S. Abu Sohel, H. Hung, R. Liu, *Angew. Chem. Int. Ed.* **2010**, *49*, 9891-9894.
- (8) Y. Shi, S. Ramgren, S. Blum, *Organometallics* **2009**, *28*, 1275-1277; A. Hashmi, C. Lothschutz, R. Dopp, M. Rudolph, T. Ramamurthi, F. Rominger, *Angew. Chem. Int. Ed.* **2009**, *48*, 8243-8246; J. Hirner, S. Blum, *Organometallics* **2011**, *30*, 1299-1302; A. Hashmi, C. Lothschutz, R. Dopp, M. Ackermann, J. Becker, M. Rudolph, C. Scholz, F. Rominger, *Adv. Synth. Catal.* **2012**, *354*, 133-147; M. Pena-Lopez, L. Sarandeses, J. Sestelo, *Eur. J. Org. Chem.* **2013**, 2545-2554.
- (9) H. Wegner, S. Ahles, M. Neuburger, *Chem.-Eur. J.* **2008**, *14*, 11310-11313.
- (10) G. Zhang, Y. Peng, L. Cui, L. Zhang, *Angew. Chem. Int. Ed.* **2009**, *48*, 3112-3115; M. Hopkinson, J. Ross, G. Giuffredi, A. Gee, V. Gouverneur, *Org. Lett.* **2010**, *12*, 4904-4907.
- (11) X. Shu, M. Zhang, Y. He, H. Frei, F. Toste, *J. Am. Chem. Soc.* **2014**, *136*, 5844-5847; D. Patil, H. Yun, S. Shin, *Adv. Synth. Catal.* **2015**, *357*, 2622-2628; J. Um, H. Yun, S. Shin, *Org. Lett.* **2016**, *18*, 484-487; A. Tlahuext-Aca, M. Hopkinson, R. Garza-Sanchez, F. Glorius, *Chem.-Eur. J.* **2016**, *22*, 5909-5913.
- (12) C. Obradors, A. Echavarren, *Chem. Comm.* **2014**, *50*, 16-28.
- (13) J. Nguyen, N. Duncan, G. Lalic, *Eur. J. Org. Chem* **2016**, *35*, 5803-5806.

- (14) N. Marion, S. Nolan, *Chem. Soc. Rev.* **2008**, *37*, 1776-1782.
- (15) M. Uehling, A. Suess, G. Lalic, *J. Am. Chem. Soc.* **2015**, *137*, 1424-1427; A. Suess, M. Uehling, W. Kaminsky, G. Lalic, *J. Am. Chem. Soc.* **2015**, *137*, 7747-7753.
- (16) T. J. Brown, D. Weber, M. R. Gagné, R. A. Widenhoefer, *J. Am. Chem. Soc.* **2012**, *134*, 9134-9137.
- (17) A. Tamaki, S. Magennis, J. Kochi, *J. Am. Chem. Soc.* **1974**, *96*, 6140-6148.
- (18) H. Peng, Y. Xi, N. Ronaghi, B. Dong, N. Akhmedov, X. Shi, *J. Am. Chem. Soc.* **2014**, *136* (38), 13174-13177.
- (19) G. A. Olah, R. Krishnamurti and G. K. Surya Prakash, In *Comprehensive Organic Synthesis*, B. M. Trost, and I. Fleming, Pergamom Press: Oxford, 1991; Vol. 3, 293-339.
- (20) For a comprehensive review of this large research area, see: Z. Dong, Z. Ren, S. J. Thompson, Y. Xu and G. Dong, *Chem. Rev.*, 2017, **117**, 9333.
- (21) K. Semba, K. Ariyama, H. Zheng, R. Kameyama, S. Sakaki and Y. Nakao, *Angew. Chem., Int. Ed.*, 2016, **55**, 6275-6279.
- (22) S. D. Friis, M. T. Pirnot and S. L. Buchwald, *J. Am. Chem. Soc.*, 2016, **138**, 8372.
- (23) X. Ma and S. B. Herzon, *J. Am. Chem. Soc.*, 2016, **138**, 8718; X. Ma, H. Dang, J. A. Rose, P. Rablen and S. B. Herzon, *J. Am. Chem. Soc.*, 2017, **139**, 5998.
- (24) S. A. Green, J. L. M. Matos, A. Yagi and R. A. Shenvi, *J. Am. Chem. Soc.*, 2016, **138**, 12779; S. L. Shevick, C. Obradors and R. A. Shenvi, *J. Am. Chem. Soc.* 2018, **140**, 12056-12068.
- (25) S. D. Friis, M. T. Pirnot, L. N. Dupuis and S. L. Buchwald, *Angew. Chem., Int. Ed.*, 2017, **56**, 7242.
- (26) For a recent example of anti-Markovnikov hydroxyridylation of alkenes using photocatalysis, see: A. J. Boyington, M. L. Y. Riu and N. T. Jui, *J. Am. Chem. Soc.*, 2017, **139**, 6582.
- (27) J. A. Gurak, Jr. and K. M. Engle, *ACS Catal.*, 2018, **8**, 8987-8992.
- (28) L. Jin, J. Qian, N. Sun, B. Hu, Z. Shen and X. Hu, *Chem. Commun.*, 2018, **54**, 5752.
- (29) N. A. Eberhardt and H. Guan, *Chem. Rev.*, 2016, **116**, 8373.
- (30) R. Cariou, T. W. Graham and D. W. Stephan, *Dalton Trans.*, 2013, **42**, 4237; L. C. Liang, P. S. Chien and P. Y. Lee, *Organometallics*, 2008, **27**, 3082; J. Breitenfeld, R. Scopelliti and X. Hu, *Organometallics*, 2012, **31**, 2128.
- (31) T. J. Anderson, G. D. Jones and D. A. Vicic, *J. Am. Chem. Soc.*, 2004, **126**, 8100; J. Breitenfeld, J. Ruiz, M. D. Wodrich and X. Hu, *J. Am. Chem. Soc.*, 2017, **139**, 13929.

- (32) Previously, Liu et al. have reported a nickel-catalyzed hydroalkylation of alkenes together with two examples of hydroarylation reaction. See, X. Lu, B. Xiao, Z. Zhang, T. Gong, W. Su, J. Yi, Y. Fu, L. Liu, *Nat. Commun.* **2016**, *7*, 11129.
- (33) F. Chen, K. Chen, Y. Zhang, Y. He, Y. M. Wang and S. Zhu, *J. Am. Chem. Soc.*, 2017, **139**, 13929.
- (34) For examples of related reductive cross-coupling reactions, see: P. Shukla, A. Sharma, B. Pallavi and C. H. Cheng, *Tetrahedron*, 2015, **71**, 2260; Q. Xurong, L. M. W. Yao, Z. J. Steve, *Angew. Chem., Int. Ed.*, 2017, **56**, 12723.
- (35) Interestingly, Zhao et al. have also reported Markovnikov selectivity in a redox neutral nickel-catalysed hydroarylation of styrenes, see: L.J. Xiao, L. Cheng, W. M. Feng, M. L. Li, J. H. Xie, and Q. L. Zhou, *Angew. Chem. Int. Ed.* 2018, **57**, 461.
- (36) J. Nguyen, A. Chong, G. Lalic, *Chem. Sci.*, 2019, **10**, 3231-3236
- (37) TEMPO has been shown to react rapidly with metal hydrides. See: A. C. Albéniz, P. Espinet, R. López-Fernández and A. J. Sen, *J. Am. Chem. Soc.*, 2002, **124**, 11278; Tempo has also been used as an oxidant in nickel-catalyzed C-H activation reactions. See: X. Wu, Y. Zhao and H. Ge, *Chem. Eur. J.*, 2014, **20**, 9530.
- (38) C. A. Tolman, *J. Am. Chem. Soc.*, 1972, **94**, 2994; R. Cramer and R. V. Lindsey, *J. Am. Chem. Soc.*, 1966, **88**, 3534
- (39) V. P. Ananikov, *ACS Catalysis*, 2015, **5**, 1964; S. A. Macgregor, G. W. Neave and C. Smith, *Faraday Discuss.* 2003, **124**, 111.
- (40) I. Buslov, F. Song and X. Hu, *Angew. Chem., Int. Ed.*, 2016, **55**, 12295; A. G. Sergeey, J. D. Webb and J. F. Hartwig, *J. Am. Chem. Soc.*, 2012, **134**, 20226.
- (41) J. J. Brunet, D. Besozzi, A. Courtois and P. Caubere, *J. Am. Chem. Soc.*, 1982, **104**, 7130.
- (42) R. H. Crabtree, *Chem. Rev.*, 2012, **112**, 1536.
- (43) Y. S. Wagh, N. Asao, *J. Org. Chem.* **2015**, *80*(2), 847-851.
- (44) G. Wang, R. Shang, Y. Fu, *Org. Lett.* **2018**, *20*(3), 888-891.
- (45) M. Barbasiewicz, M. Makosza, *Org. Lett.* **2006**, *8*(17), 3745-3748.
- (46) T. Goegsi, L. S. Soebjerg, A. T. Lindhart, K. L. Jensen, T. Skrydstrup, *J. Org. Chem.* **2008**, *73*(9), 3404-3410.
- (47) S. Wu, J. Liu, F. Liu, *Org. Lett.*, **2016**, *18*(1), 1-3.
- (48) M. D. Greenhalgh, D. J. Frank, S. P. Thomas, *Adv. Synth. Catal.*, **2014**, *356* (2-3), 584-590.
- (49) Y. Zhou, J. S. Bandar, S. L. Buchwald, *J. Am. Chem. Soc.* **2017**, *139*(24), 8126-8129.

- (50) A. J. B. Watson et al. *J. Am. Chem. Soc.* **2018**, *140*(1), 126-130.
- (51) W. Xiao et al. *Adv. Synth. Catal.* **2011** *353*(4), 617-623.
- (52) M. W. Gribble, M. T. Pirnot, J. S. Bandar, R. Y. Liu, S. L. Buchwald, *J. Am. Chem. Soc.* **2017**, *139*(6), 2192-2195.
- (53) Y. Wang, Y. Gao, S. Mao, Y. Zhang, D. Guo, Z. Yan, S. Guo, Y. Wang, *Org Lett.* **2014**, *16*(6), 1610-1613
- (54) Y. Shimada, R. Haraguchi, S. Matsubara, *Synlett.* **2005**. *26*(17), 2395-2398.
- (55) L. Chan, J. S. K. Lim, S. Kim, *Synlett.* **2011**. (19), 2862-2866.
- (56) H. Lebel, V. Paquet, *Organometallics.* **2004**. *23*(6), 1187-1190.
- (57) A. Nakamura, M. Tokunaga, *Tetrahedron Lett.* **2008**. *49*(23), 3729-3732.
- (58) S. Fortier, J. R. Walensky, G. Wu, T. W. Hayton, *J. Am. Chem. Soc.* **2011**. *113* (18), 6894-6897.
- (59) A. Di Guiseppe, R. Castarlenas, J. J. Perez-Torrent, F. J. Lahoz, V. Polo, L. A. Oro, *Angew. Chem. Int. Ed.* **2010**. *50* (17), 3938-3942.